A THEORETICAL MODEL STUDY OF LIQUID PHASE EPITAXIAL GROWTH KINETICS OF SOME TERNARY III-V COMPOUND SEMICONDUCTORS

A Dissertation submitted to the Department of Physics, Bangladesh University of Engineering and Technology, Dhaka in partial fulfillment of the requirements for the degree of Master of Philosophy in Physics

Abul Hasnat Md. Zakir Uddin

Roll No: 100014003 P
Session: October 2000

Department of Physics
Bangladesh University of Engineering and Technology (BUET)
July 2005

Acknowledgements

Without encouragements, most feasible and desirable things become difficult to achieve. One such encouragement in my life roused my enthusiasm, which resulted in the successful completion of this thesis. I am much grateful to those personalities who were the catalysts in my achievement.

I express deep sense of gratitude to my thesis supervisor **Dr. Md. Mostak Hossain**, Associate Professor, Department of Physics, Bangladesh University of Engineering and Technology (BUET) for his indispensable guidance, valuable suggestions, generous help and care and constant encouragement throughout the period of research.

I am also thankful to the Head and my teachers in the department of Physics, Bangladesh University of Engineering and Technology (BUET) for their keen interest and encouragement during the progress of this work. Also thanks to all the employees of the department.

I wish to express my indebtedness to my parents for their encouragement and support. I would like to express my gratitude to my brother in law Dr. Mizanur Rahman for his support during thesis writing. I extend gratitude to all my family members and well-wishers.

I am wholly and solely responsible for any error and omission that remained in this thesis, if any.

Abul Hasnat Md. Zakir Uddin

Abstract

For understanding the Liquid Phase Epitaxy (LPE) growth kinetics, a kinetic model has been developed for III-III-V and III-V-V compound semiconductors during the growth with phase equilibrium condition applied between the growing crystal and solution using numerical method of Laplacian centered difference approximation. Then one-dimensional diffusion limited growth models have been extended for InGaP, InGaAs and InAsP. Crystallization path and its expression was analyzed and used to understand the growth kinetics based on the phase diagram relationship. Computer programmes are used to solve different equations of layer thickness, concentration profiles, dimensionless profiles and atomic fractions. The layer thickness of the ternary compounds is grown as a function of different growth temperatures and growth times for different cooling rates. Solid composition of ternary materials as a function of temperature for different cooling rates has been calculated. The concentration profiles have also been simulated in front of growing interface for different growth temperatures and cooling rates. Dimensionless concentration parameter is also calculated and is represented as a function of different cooling rates and thickness. A comparison among the three ternaries for their respective growing thickness with time is also done. A good agreement is found between the present findings and the experimental values.

i

Contents

List of Figures

Declaration

It is hereby declared that this thesis or any part of it has not been submitted elsewhere for the award of any degree or diploma.
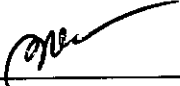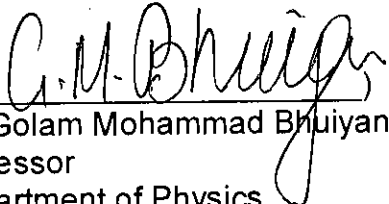
Zakir Uddin

22.07.05

Abul Hasnat Md. Zakir Uddin

Candidate

Bangladesh University of Engineering and Technology (BUET)
Dhaka
Department of Physics

Certificate of Thesis work

The thesis titled **"A THEORETICAL MODEL STUDY OF LIQUID PHASE EPITAXIAL GROWTH KINETICS OF SOME TERNARY *III-V* COMPOUND SEMICONDUCTORS"**, submitted by **Abul Hasnat Md. Zakir Uddin** Roll No: **100014003 P** Session-**October 2000** has been accepted as satisfactory in partial fulfillment of the requirements for the degree of Master of Philosophy in Physics on **10 August 2005.**

Board Of Examiners

1. (_____) Chairman
   Dr. Md. Mostak Hossain (Supervisor)
   Associate Professor
   Department of Physics, BUET, Dhaka

2. (_____) Member
   Head
   Department of Physics, BUET, Dhaka

3. (_____) Member
   Dr. Md. Abu Hashan Bhuiyan
   Professor
   Department of Physics, BUET, Dhaka

4. (_____) Member (External)
   Dr. Golam Mohammad Bhuiyan
   Professor
   Department of Physics,
   University of Dhaka, Dhaka

Dedicated To

My Parents

Chapter I

Introduction
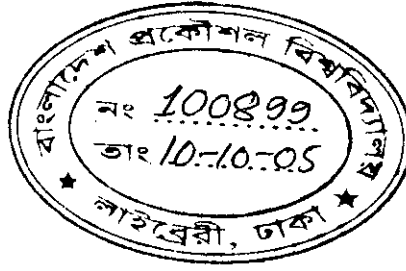
Introduction

1.1 Introduction

Several kinds of solid-state electronic devices, such as high-speed transistors and integrated circuits, are fabricated by production of an epitaxial layer of one semiconductor on a wafer of another that has a different type of electrical conductivity. Also a significance change in the performance of electronic and photonic devices has occurred on heterostructure, quantum well superlattices and other low dimensional structures in last two decades. Such kind of structures can be grown by means of epitaxial growth only.

The term "epitaxy" originated from the Greek word, which means that 'something upon' i.e. something upon a crystalline oriented substrate. Epitaxy is the deposition of a crystalline substance, usually in a thin layer, upon the surface of a single crystal of another substance. The process does not involve a chemical reaction between the two materials, but the crystalline structure and orientation of the substance determines how the epitaxial layer is deposited. In homoepitaxy a crystal is grown on a substrate of the same material. As for example, Silicon layers containing different impurity are grown on silicon substrates in the manufacture of

computer chips. Heteroepitaxy, on the other hand, is the growth of one crystal on the substrate of another e.g., gallium arsenide grown on a silicon substrate.

Epitaxial growth can reduce the growth time, wafering cost and also saved the wastages of materials during growth, cutting, polishing etc. the uniformity in the composition, controlled growth parameters and better understanding of the growth itself is the main advantages of the epitaxy. The epitaxial growth techniques have superseded the bulk growth for the fabrication of electronic circuit because the electronic circuits need only few micron dimensions.

Vapour Phase Epitaxy (VPE), Metalorganic Vapour Phase Epitaxy (MOVPE), Molecular Beam Epitaxy (MBE), Chemical Beam Epitaxy (CBE), Atomic Layer Epitaxy (ALE), Liquid Phase Electro-Epitaxy (LPEE) and Liquid Phase Epitaxy (LPE) are different types of epitaxial growth techniques. Among them, LPE is the subject of our interest because of its simplicity, low-costing and high crystalline quality. The present investigation deals with the one-dimensional numerical analysis of growth of III-V ternary semiconductors and heat transport in the melt during the LPE growth.

1.2 Different Epitaxial Techniques

1.2.1 Vapour Phase Epitaxy (VPE)

The condensation process of the material from it's own vapour is Vapour Phase Epitaxy. In VPE, the group III-V chemical compounds react with the other to form the compound semiconductor on a suitable substrate by transporting themselves from gas phase to solid-vapour interface. Here, growth is controlled by the partial pressure of each of the components of source materials. The VPE

methods of crystal growth of III-V compounds can mainly be divided into two classes: hydride vapour phase epitaxy and chloride vapour phase epitaxy.

Major advantages of VPE technique are-

i. High purity and less defect wafer can be grown from high purity charges and

ii. The epitaxial growth on large and multiple wafers are possible.

1.2.2 Metalorganic Vapour Phase Epitaxy (MOVPE)

The term 'metalorganic' refers to any compound semiconductor containing metal atoms in combination with organic radicals. The group of III metal organics [$Ga(CH_3)_3$ or $In(C_2H_5)_3$] and the group of V hydrides (PH_3 or AsH_3) introduce in the reactor by means of a carrier gas bears a result by the growth of III-V compound semiconductors. The generalized reaction for III-V compounds on MOVPE may be written as

$$R_3M + EH_3 \overset{K}{\Leftrightarrow} ME + 3RH \qquad 1.1$$

Where R=CH_3 or C_2H_5, M=group III element (Al, Ga or In) and E= group V elements (P, As or Sb). MOVPE yields high quality semi-conducting layer for fundamental semiconductor devices, both electronic and photonic.

The major disadvantages of MOVPE technique are its high cost, the use of highly hazardous starting materials and toxic the waste materials.

1.2.3 Molecular Beam Epitaxy (MBE)

The process of depositing epitaxial thin films that involves the reaction of one or more thermal beams of atoms or molecules under high vacuum condition with a crystalline surface is known as molecular beam epitaxy. To give the thermal beam of appropriate intensity, the temperature of the cells (where beams are

produced) are accurately controlled. Depending on the nature of the source used to produce thermal beams, MBE can be classified as solid source MBE and gas source MBE.

With MBE, it is possible to grow high quality (GaAs and AlAs) and multilayered structures including super-lattices with layer thickness as low as 10 $\bar{A}^0$. (Horikoshi 1986,Vaya 1989)

The disadvantage of MBE is the difficulty in growing phosphorus-containing materials as it bounces in the system. In addition, the growth alloy containing As and P is particularly difficult.

1.2.4 Chemical Beam Epitaxy (CBE)

In Chemical Beam Epitaxy growth process, beam of compound chemicals directly impinge onto a heated substrate surface. It is a technique for the growth of InP based materials with MBE. The CBE technique has been used to grow a wide range of device structure including optoelectronic devices such as InGaAsP lasers, Bragg refractors and InP based channel high electron mobility transistor.

The advantages of CBE are:

i.   The capability to grow high-quality InP-based materials.

ii. Less decomposition of source materials (AsH_3 and PH_3) are required for the growth of GaAs and InP based materials compared to MOVPE.

iii. More homogeneity and good uniformity.

iv. Vacuum in situ diagnostics.

1.2.5 Atomic Layer Epitaxy (ALE)

Atomic layer epitaxy is a well-known technique for the fabrication of compound semiconductor films. This technique utilizes either MBE or Chemical Vapour Deposition approach. In this method, a monolayer of each constituent atoms or molecule is laid down separately in place of having mixed flux at the substrate. Conditions are established when the bonds are stable. For example, in the growth of GaAs by ALE, first layer of As is deposited on the substrate and excess arsenic is swept out of the system. This layer is followed by a flux of gallium that reacts with arsenic layer, filling up sites to complete a layer of gallium and the compound GaAs. Again, excess gallium is removed from the system.

1.2.6 Liquid Phase Electro-Epitaxy (LPEE)

Liquid phase electroepitaxy is a constant growth temperature method. LPEE is initiated and sustained by passing an electric current through the solution and the substrate. The growth takes place at a constant furnace temperature and the direct current is the sole externally applied driving forces.

One of the principal advantages of LPEE is the possibility of controlling the composition of the solid phase by changing the current (Zhovnir and Zakhlenyuk 1985). Liquid phase epitaxy is one of the novel techniques for the growth of compositionally uniform, controlled thickness and low dislocation ingots of III-V compound semiconductors.

1.2.7 Liquid phase Epitaxy (LPE)

Liquid Phase Epitaxy is an important crystal growth process from both practical and fundamental viewpoints. Liquid phase epitaxy (LPE) has proven to be a versatile technique to grow semiconductor layers for material investigation and device applications. Today, in spite of the availability of highly sophisticated epitaxial techniques like MBE, CBE and MOVPE, the exploration and development of many devices are still carried out using LPE (Kuphal 1994). This is essentially due to the simplicity of the technique, high crystalline quality of the grown thin films and inherently less harmful to the environment because the raw materials and the waste products are less toxic and not pyrophoric than that of the other techniques. The present work is based upon the LPE. The LPE process is discussed in details in Chapter two.

In the present work a one-dimensional diffusion limited equation for the growth of LPE using numerical method is studied. Crystallization path is also studied. Then concentration profiles, layer thickness as a function of time and temperature and dimensionless concentration profiles are constructed. Finally the theoretical findings have been compared with the experimental values.

The process of
Liquid Phase Epitaxy

2.1 Introduction

LPE growth takes place on a substrate immersed in supersaturated solution. This technique is convenient for the growth of III-V compound semiconductors. In this process, the solvent element of the constituent of the growing solid (e.g. In or Ga) is incorporated into the solid only as a dopant. The solvent contains a small quantity of a solute (e.g. As in Ga), which is transported towards the liquid-solid interface. The process is controlled best if this transport occurs only by diffusion i.e. the driving force in the solution is a concentration gradient of the solute. So, Liquid Phase Epitaxy (LPE) means the growth of thin films from supersaturated metallic solution on a crystalline oriented substrate (Kuphal 1994). The growth boats are commonly designed such that, essentially, only diffusion perpendicular to the interface occurs; convection and surface tension related transports are suppressed. Convection and surface tension related transports are suppressed by taking temperature gradient as small as possible and utilizing larger lateral dimension of the substrate compared to the height and radius of the curvature of the solution. Applying these constrains, the LPE process can be treated as one

dimensional diffusion process with diffusion limited growth rate. In LPE growth process, the relationship between the temperature and the solubility as predicted by the phase diagram has to be utilized for the analyzing of the growth process. LPE technique consists of four mechanisms as-

i) Saturated solution is prepared containing a quantity of solute at the saturation temperature.

ii) By cooling the saturated solution, supersaturated solution is obtained.

iii) For required layer of thickness, contact between substrate and the solution is done for appropriate time.

iv) Removing the substrate from the solution terminates the growth.

2.2 Classification of LPE

The LPE growth is generally classified as-

a) Tipping technique
b) Dipping technique
c) Sliding technique and
d) Sandwich technique

a) Tipping technique

In tipping technique, the substrate is held tightly at the upper end of a graphite boat and the growth solution is placed at the other end. Nelson (1963) first introduced the tipping device where whole furnace and quartz tube had to be tipped. By tipping the furnace, the solution is brought into contact with the substrate. Then an epitaxial layer is grown by slowly cooling the furnace. After growing the desire thickness of the epitaxial layer, growth is terminated by tipping the furnace back to the original position. Figure 2.1 shows a schematic diagram of

the tipping technique of LPE system. Bauser et al (1974) modified the Nelson's tipping LPE technique as shown in figure 2.2(a), where the quartz tube including the crucible is tipped around the longitudinal axis. Excellent layer purity is produced with this technique due to very simple design of the boat and rather thin graphite wall. Since, no sliding of graphite parts occurs so that no dust particles can be introduce by abrasion.

The disadvantage of the tipping techniques are-

i) The thickness homogeneity is only due to two-dimensional diffusion in the solution.

ii) Only single epitaxial layers can be grown and

iii) The solution cannot be protected against evaporation of the volatile elements.

To overcome the restriction of growing multilayer, Kaufmann and Heim (1977) developed a technique to grow multilayer, which is a combination of tipping and slider as shown in figure 2.2(b). In this case, the solution is brought into the substrate by tipping. A slider transports the substrate from one compartment into the next when the solution is not in contact with the substrate. To start and stop the deposition, the constructions have to be rotated forward and backward in these techniques. As a consequence, thin layers are tapered, because the solution rests for a longer time on one side of the substrate than the other. With improve version of the tipping-slider boat (Kuphal 1994) this disadvantage was overcome, which can be rotated by 360^0 as shown in figure 2.2(c).
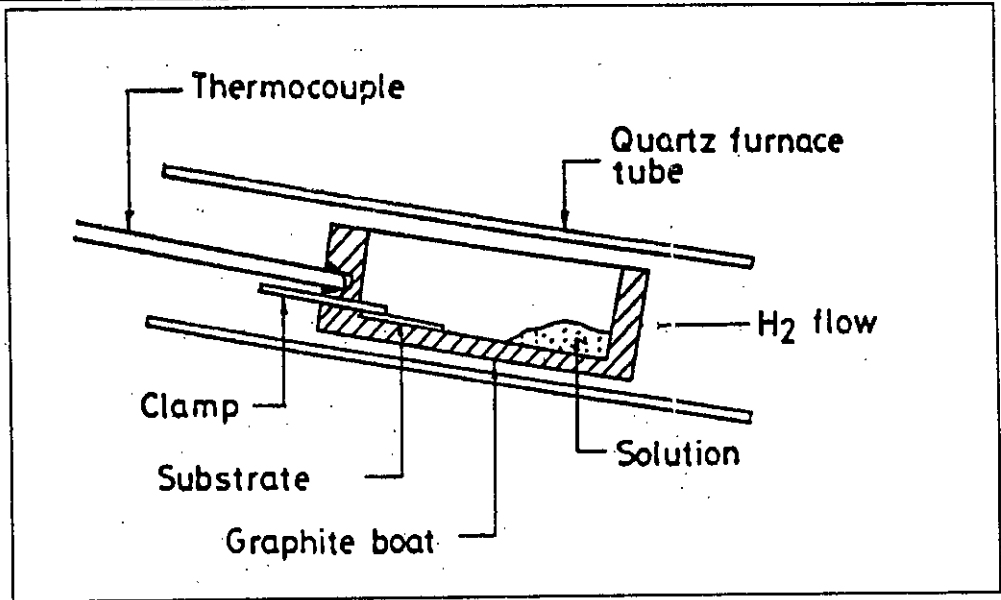
Figure 2.1: Schematic diagram of the tipping technique of LPE growth system.
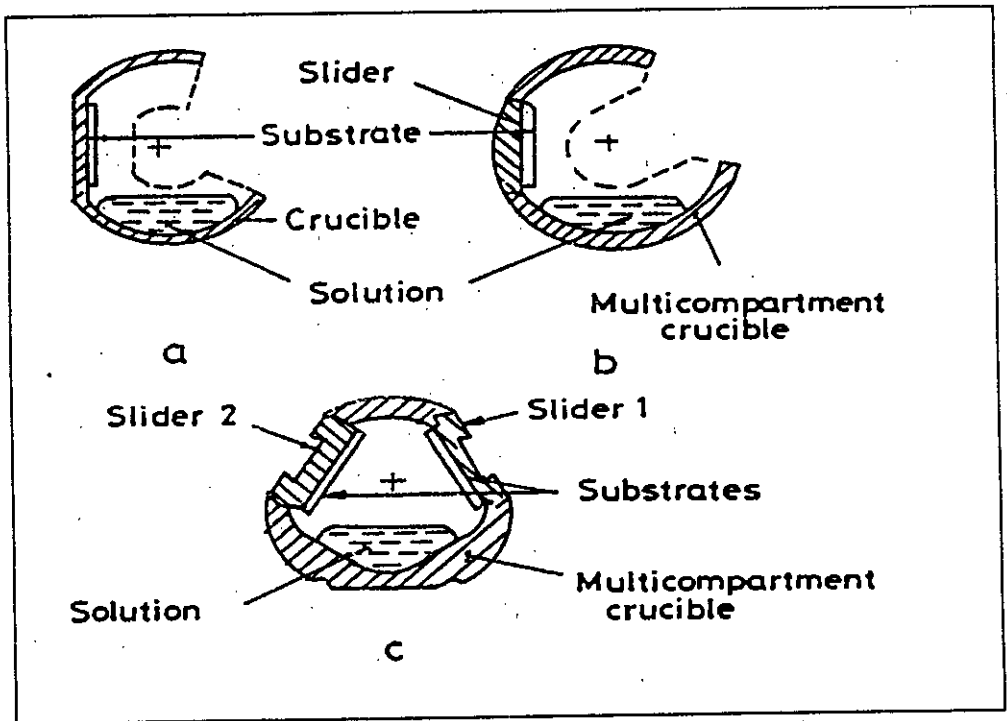
Figure 2.2: Different designs of tipping boat- a) a simple tipping boat, b) a combination between a tipping and a slider boat, c) a tipping slider boat with the ability to be rotated by 360^0.

b) Dipping technique

The dipping technique consists of a vertical furnace and growth tube with the graphite crucible containing the solution at the lower end as shown in figure 2.3. Initially the substrate fixed in a movable holder is positioned above the solution. Growth is initiated by immersing the substrate in the solution at the desired growth temperature and terminated by withdrawal of the substrate from the solution. The main disadvantage in this technique is that thickness is not homogeneous.

Two German manufacturers improved the dipping technique for multiwafer growth. In this case, a horizontal furnace and two large-volume horizontal solution containers are used. One hundred parallel-positioned 2-inch wafers are simultaneously dipped into one solution. The solution is used only once, but can be recycled. This technique allows the growth of double layers and it is extremely well suited for the mass production of LED wafers, where thickness homogeneity is not so important (Kuphal 1994).

c) Sliding Technique

The sliding technique is one of the most frequently used techniques used for the growth heterostructures, for example as in laser diodes. The sliding technique is the horizontal multibin-slider system, which is useful for the growth of multilayered structures (Panish et al 1970). In the simplest case, the boat consists of a substrate holder with the substrate in a recess and the slider containing the differently composed solutions in its bins as shown in figure 2.4. (Kuphal 1994). As the solution generally do not stick to purified graphite, they can
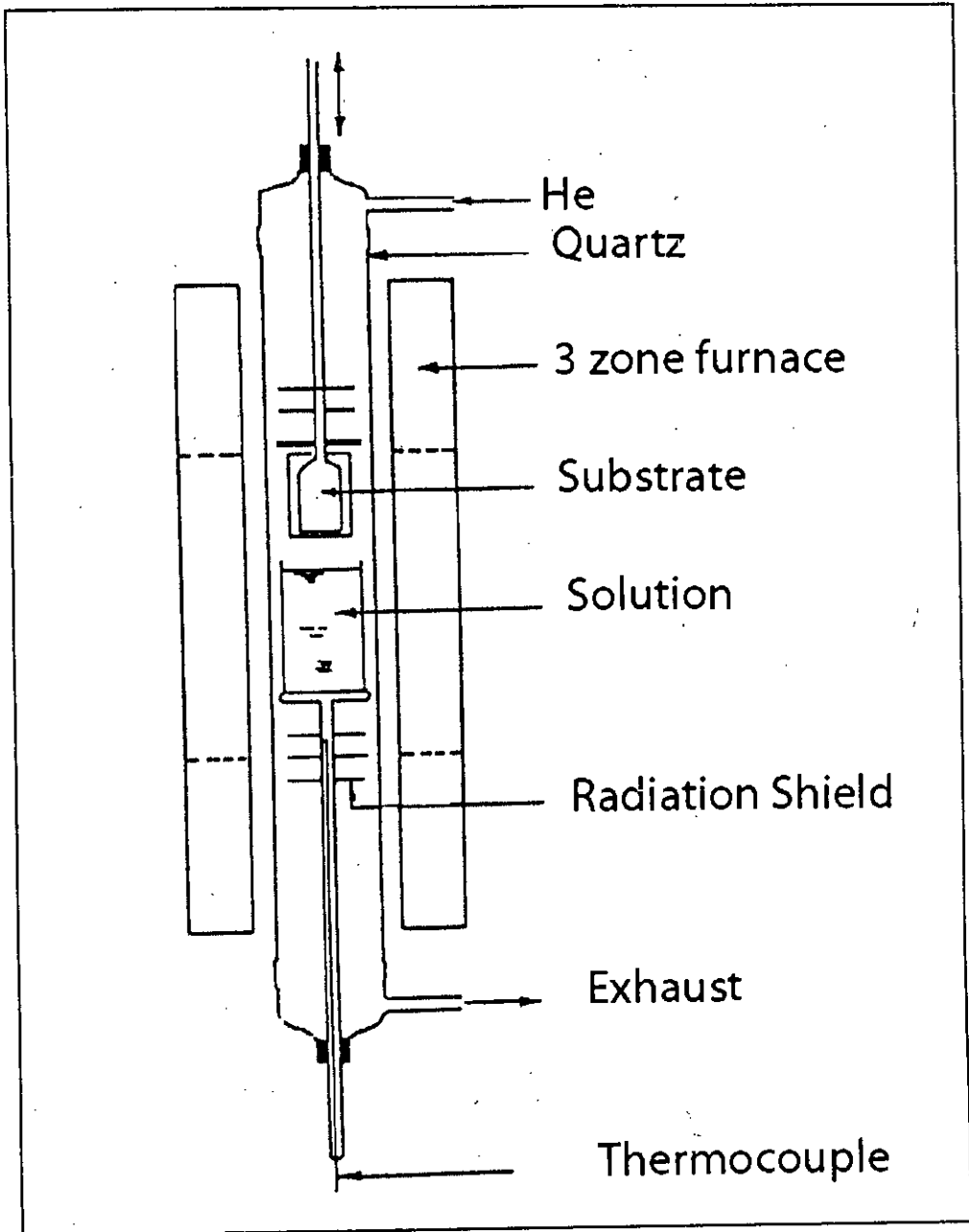
Figure 2.3: LPE growth apparatus employing the dipping technique.
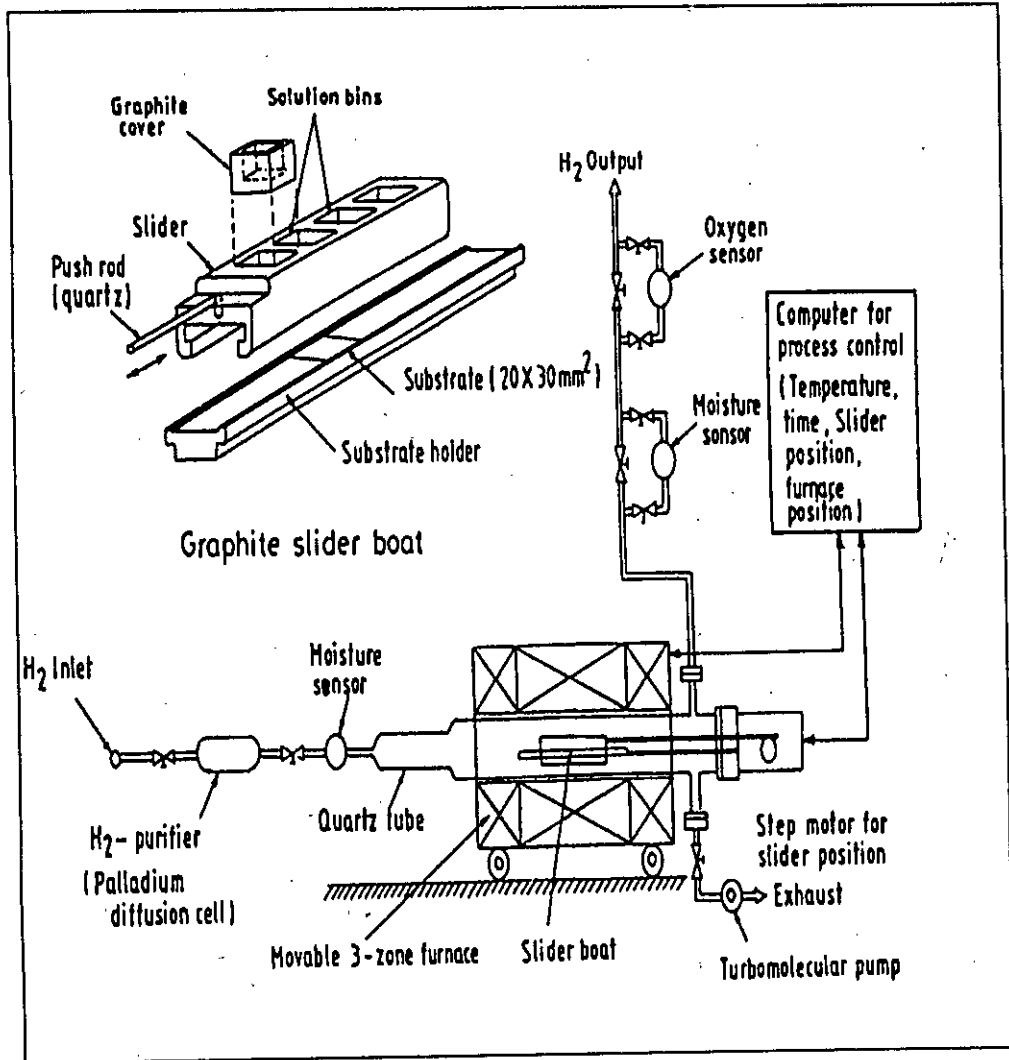
Figure 2.4: Schematic view of horizontal multibin-slider LPE system

be wiped off the substrate by the graphite walls of the slider to terminate the growth. A horizontal fused silica push rod moves the slider, which is actuated by hand or computer controlled stepper motor. The pushing direction is forward and backward allowing the growth of multilayer from two neighboring solution. The minimum growth time required for a single layer is achieved about tenth of a second. Each solution is usually protected by a graphite cover, which prevents evaporation and contamination. Mostly in the slider boat designs, it causes the wetting problems to grow at lower temperatures. Piston boat design is used to overcome these problems shown in figure 2.5. The advantage of the piston boat LPE system is that the solution used for the growth of one layer is pushed out by the solution used for the growth of next layer and is collected in a disposal bin.

d) Sandwich technique

The sandwich growth cell configuration is shown in figure 2.6 and was investigated by Sukegawa et al (1988), which consists of two horizontal substrate sets face to face and kept 4mm apart in a graphite boat. By gradually lowering the temperature the growth proceed to maintain the supersaturation after including a saturated solution between the substrates. The solution is gradually depleted of solute in the vicinity of a growing substrate. In general, the solute-depletion convection is a spatially non-uniform time dependent macroscopic phenomenon. The conservation of mass, balance of linear and angular momentum of energy governs the macroscopic phenomenon along with the LPE. Moreover, the principle of conservation of mass of solute species must also be invoked, since the solution is assumed to be a binary fluid mixture (Kimura 1994).

Figure 2.5: Schematic diagram of a piston type slider boat.
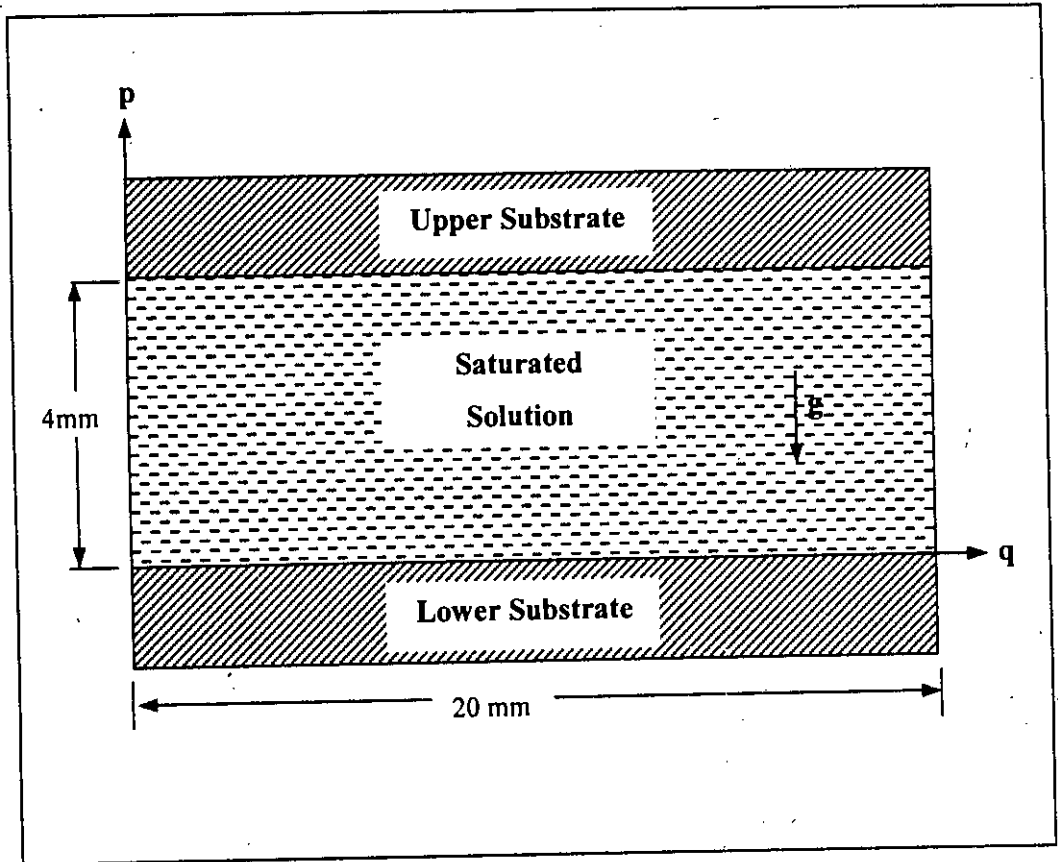
Figure 2.6: LPE growth cell configuration for sandwich technique.

Kanai (1997) described the experimental results, where numerical simulation was performed in a sandwich cell. The results of the simulation showed that the higher dissolution rate on the lower substrate and higher growth rate on the upper substrate are a consequence of solute convection.

2.3 Advantages of LPE technique

1. Very low cost of building a basic LPE growth system and with little modification almost all kinds of possible semiconductors can be grown.

2. As it is an equilibrium growth process, growth-in defects are minimum. Thick layer can be grown very easily due to higher growth rate.

3. The LPE growth process is inherently less harmful to the environment than other techniques due to high deposition efficiency and also the growth materials are relatively safe t o handle.

4. LPE is well suited a an industrial process, especially for the production of green GaP LEDs, red AlGaAs LEDs and GaAs IREDs because of low cost and device performance.

5. For the fabrication of high quantum efficiency optoelectronic devices, LPE-grown materials are best suited.

6. The LPE growth technique is much more sensitive to the substrate orientation than the other epitaxial technique, since it is being a near-equilibrium process.

7. Many ternary and quaternary compound semiconductors containing volatile materials can be easily grown by LPE.

8. The grown materials in LPE process have good reproducibility uniformity.

2.4 Disadvantages of LPE technique

1. LPE is considered to be applicable only for the production of single devices but not for integrated circuits.

✳2. A miscibility gap occurs in certain alloy systems when produced by LPE but not by other epitaxial method.

3. LPE technique is not suitable for producing devices based on strained layers.

4. Controlling the growth of each monolayer by a periodical interruption of the group III and group V fluxes as in ALE is not possible with LPE technique.

5. The growing LPE epilayer surface is hidden by the metallic solution hence an in-situ characterization of growing is not possible.

6. For the production of device structures involving thin layers, superlattice or quantum well, LPE appears to be not suited. This is essentially due to the moderate thickness control of thin layers.

2.5 Review of literature on LPE

H. Nelson of Bell laboratories demonstrated the LPE technique first in 1963 by fabricating Ge tunnel diodes and GaAs lasers. Currently the use of LPE has been mainly concentrated on the growth of III-V compound semiconductors and its ternary and quaternary alloys. III-V compound semiconductors have received much attention due to their uses in fabrication microwave and optical

devices. Many 'first' of electronic and optoelectronic devices were based on LPE structure such as LEDs, lasers, photodetectors and solar cells. Later this technique was successfully used to make high-speed electronic devices like Gun diodes, Field-effect transistor and heterojunction bipolar transistors.

The earliest applications from the grown materials by LPE are the visible LEDs. Green LEDs based on GaP and photoluminence intensity emission wavelength was 0.57μm (Beppu et al 1977). Parry and Krier (1994) have grown In$_{0.97}$Ga$_{0.03}$As on p-type InAs substrate by LPE for making light emitting diodes. These devices exhibit efficient infrared methane gas sensors for the cost effective detection and monitoring of methane gas in various application.

Chen and Wu (1995) from the research institute of electrical Engineering National Tsing Hua University, China have grown InGaAsP epitaxial layers by LPE using a horizontal sliding boat system and fabricated orange light-emitting diodes. Sun et al (1996) from the same institute have obtain high quality GaSb layer grown from Sb-rich soluion by LPE and fabricated GaSb photodiodes which exhibits a low dark current of 2μA at -5V.

Mao and Krier (1996) of Advance Materials and Photonics , Lancaster University, UK have developed InAsSb on (100) p-type GaSb substrate based on LPE technique and observed electroluminescence intense emission near 1.2μm at room temperature.

The advantage of using III-V materials for photodetector applications compared to Si and Ge, are that, the band gap of the material can be suitably chosen for a particular wavelength region. Many III-V materials are direct band

gape type, offering high quantum efficiency and their high mobility gives the possibility of high-speed application. Major kinds of photodetectors are of photodiode type. Some examples of photodetectors for longer wavelengths made for the first time LPE are the pin-photodiodes from the systems of InGaAsP/InP (Wieder et al 1977) and InGaAs/InP (Leheny et al 1979).

Panish et al (1970) at Bell Laboratories have developed double-heterostructure AlGaAs/GaAs laser diode continuous-wave (CW) lasing at room temperature. Also the continuous-wave (CW) operation of double-heterostructure (DH) lasers emitting at wavelength beyond $1\mu m$, realized in the systems of InGaAsP/InP (Hsieh et al 1976). Katz et al (1980) have reported a new device involving monolithic integration of an injection laser and heterojunction bipolar transistor GaAlAs grown GaAs substrate attractive in high-speed optical communication system. The exploration and development of many materials and devices were only possible due to the existing LPE technique so that many years were saved prior to the advent of other epitaxial technique (Kuphal 1994).

One of the most challenging problems in heteroepitaxy is the growth of layers with thickness smaller than the electron free path, i.e. of around 10nm. Some of the examples of grown thin layers by LPE are found (Ohki et al 1987; Tanaka et al 1989), including doping superlattice (Konig and Jorke 1985; Greene et al 1987), but most of them not exceeding thickness 15nm. LPE fabricated MQW laser diodes reported only in very few reports (Dutta et al 1985; Sasai et al 1986; Krier and Mao 1995).

High efficiency solar photovoltaic cell based on CdTe and GaAs is another area where LPE holds great promise and Russians have made great progress in this area using modified LPE techniques. Milanova et al (1999) have studied spectral characteristics of GaAs solar cells grown by low-temperature LPE and obtained conversion efficiency from the optimized cell under one-sun AM 1.5 global illumination is about 23.4%.

Zhuravlev et al (1998) have grown p-GaAs: Zn (100) epitaxial layers by LPE from gallium and bismuth melt. This epitaxial layer of heavily zinc-doped GaAs is widely used in the fabrication of photocathodes with negative electron affinity and in the base layer of heterobipolar transistors.

A number of excellent reviews on the LPE technique have already written by several authors (Kressel and Nelson 1973; Casey and Panish 1978; Benz and Bauser 1980; Stringfellow 1982; Astles 1990; Kuphal 1994). In the past few years there have been many new developments in LPE, which makes this technique attractive for the future as well. These includes automation of the growth process for better layer thickness control, melt casting systems to facilitate the work of weighing the source materials, larger wafer areas up to 510nm in diameter, multiple-wafer boat construction, better control of the layer morphology and a deeper theoretical understanding.

Peev N.S. (1999) worked on theoretical understanding of behavior of n-component during the LPE growth. He showed that two types of components, with positive and negative concentration gradient, are present in LPE growth process, For components with positive concentration gradient, supersaturation occurs

above the substrate whereas, for deposition of the components having a negative concentration gradients, liquid phase is superheated.

Gao H H et al (1999) reported the growth of very pure InAs epitaxial layers of high quantum efficiency, by introducing the rare-earth element Gd into the liquid phase during LPE growth and found that the carrier concentration of InAs layers can be effectively reduced up to 6×10^{15} cm^{-3}. Also, the peak photoluminescence (PL) intensity of such layers can be considerably increased by between ten- and 100-fold compared with untreated material.

Recently, Berger S. et al (2001) has performed liquid phase epitaxial growth of silicon on porous silicon for photovoltaic applications and Aichele T. et al (2003) showed that high quality Garnet layers could be prepared by liquid phase epitaxy for microwave and magneto-optical applications.

Chapter III

Growth kinetics of LPE

Growth kinetics of LPE

3.1 Introduction

Nucleation is the birth stage of epitaxial growth. Nucleation can often be introduced by external influence like agitation, mechanical shock, friction, extreme pressure, electric and magnetic fields, spark discharge, ultraviolet, x-rays, γ-rays, sonic and ultrasonic irradiation and so on. Recently, it has become possible in favorable cases to measure the actual nucleation rates and their variation with supersaturation and temperature (Adams et al 1984). A brief study of the nucleation kinetics, modeling of one dimensional solute diffusion growth theory and the LPE growth process are given in this chapter.

3.2 Nucleation kinetics

In nucleation, the initial fragments of a new and more stable phase capable of developing spontaneously into gross fragments of the stable state are initiated. So, nucleation is consequently a study of initial stages of the kinetics of such transformation and must exist on the substrate surface to occur LPE growth. The nucleation is initiated at the interface between the melt and the substrate; a composition gradient is established within the melt, driving more materials to the interface. At every point of the interface, the composition gradient within the melt

must have the same value and must be perpendicular to the substrate. Nucleation, like ordinary chemical kinetics, involves an activation process leading to the formation of unstable intermediate stages of embryo. If the embryo grows to a particular size i.e. critical size, then there is a greater probability for the nucleus i.e. critical nucleus to grow. Thus the birth of critical nucleus is an important event in the crystal growth and nucleation is the precursor of crystal growth and of the overall crystallization process (Michael et al 1965). The critical nucleus process result from the excess of surface energy that is sufficient to produce the aggregate as a new phase in the presence of mother phase (Chernov et al 1984).

Nucleation may occur spontaneously or induce artificially. For spontaneously occurrence, it is called homogeneous and for artificial introduction, it is termed as heterogeneous. If the nucleus is formed homogenously in the interior of the parent phase, it is called homogenous nucleation. On the other hand if the nuclei form heterogeneously around ions, impurity molecules or on dust particles on the surface or at structural singularities such as dislocation or other imperfections, it is called heterogeneous nucleation.

3.2.1 Free Energy of formation of a spherical nucleus

Super saturation plays an important role in the nucleation process and is the main factor controlling the rate of nucleation. The formation of a liquid micro-cluster from the supersaturated vapor or a solid micro-crystal from the liquid demands a certain quantity of energy to be spent in the creation of the new phase. Once the embryo of the new phase is created, it will have energies associated with

its volume and surface. Let ΔG is the overall excess free energy of the embryo, then the free energy of the formation of a nucleus can be written as

$$\Delta G = \Delta G_S + \Delta G_V \qquad\qquad 3.1$$

where ΔG_S is the surface excess free energy (positive) and ΔG_V is the volume excess free energy (negative quantity).

The free energy of formation for a spherical shape of nucleus of radius r, can be expressed as (Hossain et al 1999a),

$$\Delta G = 4\pi r^2 \sigma + \frac{4}{3}\pi r^3 \Delta G_v \qquad\qquad 3.2$$

where σ is the crystal-solution interfacial tension and ΔG_v, which is related to supersaturation or super-cooling, is the free energy change of the transformation per unit volume. Since the surface energy term increases with r^2 and the volume term decreases with r^3, the total free energy increases in the size of the nucleus, attains the maximum and decreases for the further increase in the size of the nucleus as shown in figure 3.1

The size corresponding to maximum change in the free energy is known as the critical radius and can be obtained by maximizing equation (3.2)

$$\frac{d(\Delta G)}{dr} = 0 \qquad\qquad 3.3$$

According to the classical theory of capillarity approximation, the surface tension is assumed to be independent of the size of the nucleus. Hence, the size of the critical nucleus is

$$r^* = -\frac{2\sigma}{\Delta G_v} \qquad\qquad 3.4$$
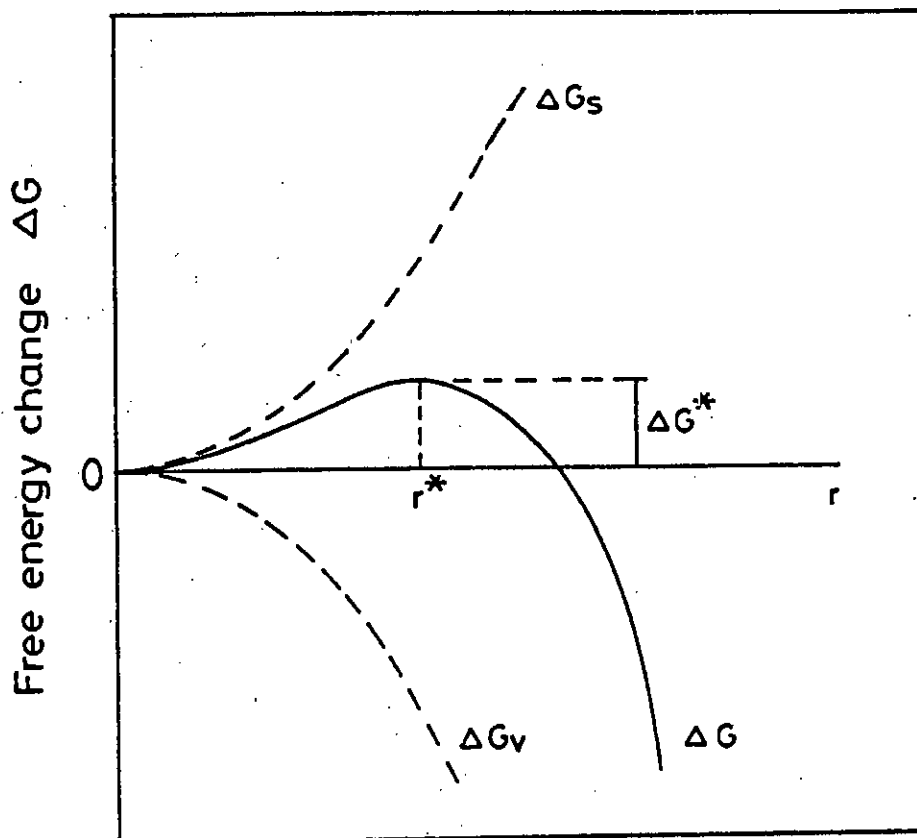
Figure 3.1: Dependence of surface free energy change, ΔG_S, volume free energy change, ΔG_V and the net free energy change, ΔG for the size, r of the nucleus.

Substituting the value of r* from equation (3.4) in equation (3.2), the free energy change associated with the formation of a critical nucleus is obtained as

$$\Delta G^* = \frac{16\pi\sigma^3}{3(\Delta G_v)^2} = \frac{4}{3}\pi\sigma(r^*)^2 \qquad\qquad 3.5$$

If there are n molecules per unit volume, the concentration of nuclei of critical size can be expressed as,

$$n^* = n\exp\left(-\frac{\Delta G^*}{kT}\right) \qquad\qquad 3.6$$

where ΔG^* is the total Gibbs free energy change for the formation of the critical nucleus, k is the Boltzman constant and T is the absolute temperature.

According to classical theory, the number of critical nuclei formed per unit time per unit volume is known as the rate of nucleation and is given by-

$$I = A\exp\left(-\frac{\Delta G^*}{kT}\right) \qquad\qquad 3.7$$

where I is the nucleation rate and A is a pre-exponential factor.

3.3 Theory of Diffusion limited growth

In liquid phase epitaxy, solute elements are transported towards the growth interface mainly by diffusion during growth process. To comprehend the growth kinetics of the epilayers, the information of concentration gradient of the solute atoms in front of the growing crystal solution interface is very essential. Theoretical modeling and computed method plays a key role in analyzing the kinetics of growth process and are aimed to make experimental research more accurate and efficient. Preliminary computations are often helpful for the design of experimental apparatus and understanding of the growth process.

3.3.1 One dimensional diffusion limited growth

Diffusion limited growth theory in one dimensional approach has widely been used to explain the LPE growth kinetics for a wide range temperature and different growth techniques (Crossley and Small 1971; Crossley and Small 1972; Pan et al 1986; Traeger et al 1988; Dobosz and Zytkiewicz 1991; Dizaji and Dhanasekaran 1996a). Based on this theory, the LPE growth of some binaries (InAs, GaAs, InP, etc) and ternaries (InGaP, GaAsP, AlGaAs etc.) of III-V compound semiconductors materials have already been numerically simulated. Details of the one dimensional diffusion growth theory are given as follows.

3.3.1.1 One dimensional mathematical model

The diffusion-limited growth is possible only when the interface kinetics is extremely fast. One dimensional solute diffusion equations are given for the growth of binary III-V compound (Astles 1990) as

$$\frac{\partial C(p,t)}{\partial t} = D\frac{\partial^2 C(p,t)}{\partial p^2} + R_V \frac{\partial C(p,t)}{\partial p} \qquad\qquad 3.8$$

where C(p,t) is the solute concentration in the binary solution, p is the distance in the solution from the solid-liquid interface and perpendicular to the substrate, t is the growth time, D is the diffusion coefficient of solute atoms in the solvent, and R is the interface velocity (by which the interface move into the solution).The interface velocity is low enough that the term $R_V\{\partial C/\partial p\}$ in equation (3.8) is negligible (Moon et al 1974).

Therefore the equation (3.8) can be expressed as

$$\frac{\partial C(p,t)}{\partial t} = D \frac{\partial^2 C(p,t)}{\partial p^2} \qquad\qquad 3.9$$

The solute atoms may not diffuse independently inside the melt in case of ternary solution, so a single diffusion coefficient is not sufficient to describe the diffusion phenomenon and as a result equations become more complex. The diffusion coefficient has to be replaced by a diffusion coefficient matrix in which the elements are D_{ij} (where i and j are the components in the multicomponent solution). Each component may experience the driving force due to the gradient of all components in the system. Non-diagonal elements of the diffusion matrix D_{ij} seem to be negligible for dilute solution used in LPE, since the interaction between the dilute components is very small and so non-diagonal elements are usually taken to be zero (Kuphal 1994).

Hence, a model equation of one dimensional for ternary element relative to the interface can be written as

$$\frac{\partial C_u(p,t)}{\partial t} = D_u \frac{\partial^2 C_u(p,t)}{\partial p^2} \qquad\qquad 3.10$$

where $C_u(p,t)$ is the concentration of solute atoms in the dilute solution at the given instant and D_u is the diffusion coefficient of the respective solute atoms in the solution along the p-axis and 'u' is the solute atoms in the solution.

3.4 LPE growth process

In LPE growth, the system is initially heated above the saturation temperature, T_s, in order to obtain a homogeneous mixture of the solution constituents. Then it is cooled down, and the substrate is brought into contact with

the solution at the starting temperature T_A. The growth is then terminated at the end temperature, T_{END}, by removal of the substrate and the furnace is subsequently cooled down quickly to avoid any thermal degradation of the grown layer (Kuphal 1994). There are three important LPE growth techniques namely: the equilibrium cooling technique, step-cooling technique and super-cooling technique. The typical temperature-time profiles during the different LPE growth process are shown in figure 3.2.

To find out the equations of epitaxial layer thickness as a function of growth time for different LPE growth techniques from the solution of the solute diffusion equation, we have considered the following principal assumptions:

1. There is no solute diffusion in the solid phase

2. During the growth, at any given instant the solute concentration in the solution at the growth interface is given by the liquidus curve i.e. the liquid and solid are in equilibrium at the interface.

3. The solute concentration at the free surface of the solution does not change during a growth run i.e. the solution is semi infinite.

4. The diffusion coefficient and the slope of the liquidus curve are temperature dependent function for some ternary compounds.

Some authors (Moon 1974; Hsieh et al 1974; Hossain Md. Mostak 1999a) have developed the equation for epitaxial layer thickness as a function of time for binary compounds by solving one dimensional solute diffusion equation with appropriate boundary condition. Kuphal (1994) has derived the equation for layer

thickness as a function of time for many component systems by solving one dimensional solute diffusion equation with appropriate boundary conditions. An equation for epitaxial layer thickness as a function of time for binary compound are derived here for the different LPE techniques by using the solution of one dimensional solute diffusion equation in cases of semi-infinite growth solution and finite growth solution.

3.4.1 Equilibrium-cooling technique

In equilibrium cooling technique, the starting temperature is equal to saturation temperate T_S. The solution is brought into contact with the substrate at T_S and the system is linearly cooled to an end temperature at a constant cooling rate. At T_S, the solution contains uniform concentration C_0, i.e. C (p, 0)=C_0 for all position of p and then it is cooled at a constant cooling rate, α, such that

$$T = T_s - \alpha t \qquad\qquad 3.11$$

At the time of growth, for small cooling intervals, the equilibrium solute concentration C_E is a linear function of temperature T_E, i.e., m=dT_E/dC_E. Here m is the slope of liquid curve equal to $\Delta T/(C_0-C_1)$, C_0 is the initial concentration given by the liquidus curve at temperature T_S and C_1 is the concentration given by the liquidus curve at the temperature of T_S-ΔT and ΔT is the degree of super-cooling. For equilibrium cooling technique the boundary conditions are

$$C(p,0) = C_0 \text{ and } C(0,t) = C_0 - \frac{\alpha t}{m} \qquad\qquad 3.12$$

Using these boundary condition and for a semi-infinite growth solution, the equation for the thickness of the epitaxial layer as a function of time
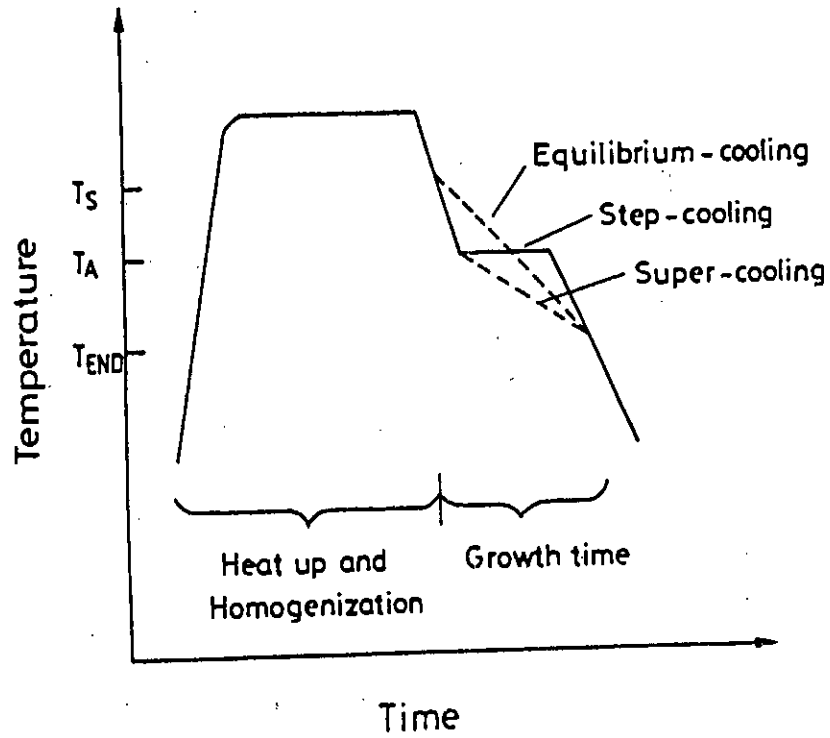
Figure 3.2: Typical temperature-time profile during Epitaxy.

for equilibrium cooling technique can be derived as (Moon 1974; Hsieh 1974),

$$d_\alpha(t) = \frac{4}{3}\left(\frac{\alpha}{C_S m}\right)\left(\frac{D}{\pi}\right)^{1/2} t^{3/2}$$
3.13

where d is the layer thickness, D is the diffusion coefficient of solute atoms in the solvent and C_S is the solute concentration in the grown layer(solid).

3.4.2 Step-cooling technique

The substrate and the solution are cooled separately at a constant rate from saturation temperature, T_S, till spontaneous precipitation formed in the solution in the step-cooling technique. When precipitation starts to form in the solution at a particular temperature T_A, temperature is kept constant and the substrate is brought into contact with solution until the desired layer thickness is grown.

For step-cooling technique the boundary condition are

$$C(p,0) = C_0 \text{ and } C(0,t) = C_1$$
3.14

where C_1 is the solute concentration given by the liquid curve at $(T_S\text{-}\Delta T)$ is the amount of super-cooling and it is small enough to avoid the occurrence of homogeneous nucleation in the solution. Hence the boundary condition can be expressed as

$$C(0,t) = C_1 = C_0 - (C_0 - C_1) = C_0 - \frac{\Delta T}{m}$$
3.15

The equation for the thickness of epilayer as a function of time for step-cooling technique can be found as (Moon 1974; Hsieh 1974)

$$d_\Delta(t) = 2\Delta T\left(\frac{1}{C_S m}\right)\left(\frac{D}{\pi}\right)^{1/2} t^{1/2}$$
3.16

3.4.3 Super-cooling technique

Super-cooling technique has the same initial conditions as step-cooling technique, where both the substrate and the solution are cooled separately at a constant rate α from the saturation temperature T_S to T_A and then contact is made between them. But like equilibrium cooling technique, the system is further cooled at the same rate until the growth is terminated. Therefore, super-cooling technique can be considered as a combination of step-cooling technique and the equilibrium cooling technique.

For super-cooling technique, the boundary conditions are-

$$C(p,0) = C_0 \text{ and } C(0,t) = C_1 - \frac{\alpha t}{m} = C_0 - \frac{\Delta T}{m} - \frac{\alpha t}{m} \qquad 3.17$$

where C_0 is the initial concentration of solute in the solution, α is the constant cooling rate, m is the slope of the liquidus curve, ΔT is the amount of super-cooling and t is the growth time. With these boundary conditions and a semi-infinite growth solution, the layer thickness as a function of time is given by (Feng et al 1980) as

$$d(t) = \left(\frac{1}{C_s m}\right)\left(\frac{D}{\pi}\right)^{1/2}\left(2\Delta T t^{1/2} + \frac{4}{3}\alpha t^{3/2}\right) \qquad 3.18$$

or $\quad d(t) = d_\Delta(t) + d_\alpha(t)$ $\qquad\qquad\qquad$ 3.19

The super-cooling technique is a combination of step-cooling technique and equilibrium technique, which was experimentally proved by Hsieh (1974) for GaAs and Kao and Eknoyan (1983) for GaP.
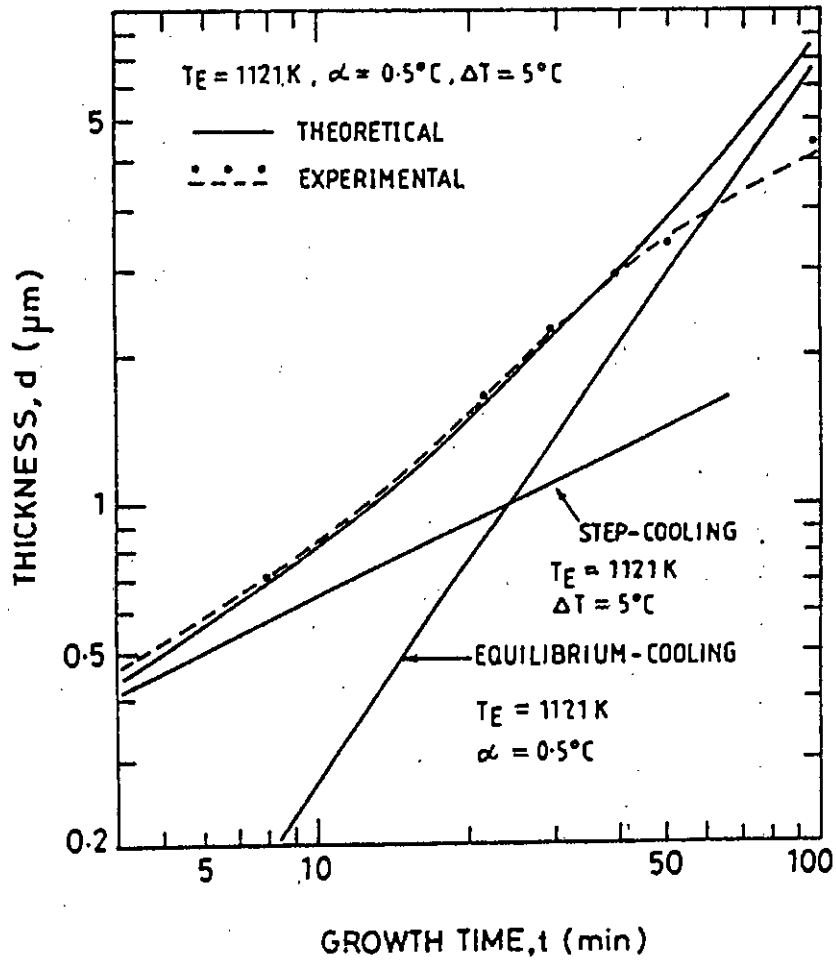
Figure 3.3: Thickness of the GaP LPE layer grown at 1121K as a function of time with different cooling technique (Kao and Eknoyan 1983).

Figure 3.3 represents the thickness as a function of growth time for GaP grown for different cooling technique shows that experimental results are very close to the theoretical line for step-cooling growth, where as the higher units of time, they come closer to that for equilibrium cooling growth.

Chapter IV

Growth kinetics of Ternary III-V Compound

Semiconductor in LPE

Growth kinetics of Ternary III-V Compound Semiconductor in LPE

4.1 Introduction

Liquid Phase Epitaxy (LPE) uses the solution method to grow crystals on a substrate. The substrate is placed in a solution with a saturated concentration of solute. This technique is used to grow many crystals employed in modern electronics and optoelectronic devices. Liquid phase epitaxial growth kinetics of III-V ternary alloy semiconductors provides useful information about the suitable growth conditions for growing an excellent quality thin layer. The growth temperature is very important for the growth of high quality epitaxial layers for material investigations and device application. One of the advantages of ternary alloys over binary semiconductors is the possibility of varying the band gap by changing their alloy composition.

For the growth of ternary alloys with LPE, the solution containing the atomic fraction x_u of its constituents, where $\sum x_u = 1$ and the solution are kept in equilibrium at initial temperature T_E. A substrate, normally one of the binary compounds, which makes up the ternary alloy, is brought in contact to a slightly super-cooled solution. By gradually lowering the temperature of substrate, an ultra thin layer of ternary solid deposited over the substrate.

A theoretical model is proposed to simulate the composition variation of ternary system of type III-III-V and III-V-V compound semiconductors during the LPE growth in present work. $In_{1-x}Ga_xAs$ and $In_{1-x}Ga_xP$ are taken as example of III-III-V group and $InAs_xP_{1-x}$ is taken as example of III-V-V systems in our simulation study. Also crystallization (solidification) path concept has been used to construct concentration profiles, where expression for the equilibrium atomic fraction of one of the solutes in each ternary system has been obtained. Here flux of each species in ternary is considered to be proportional to its constituent solid mole fraction at any time.

4.2 Growth kinetics of ternary system

4.2.1 One dimensional mathematical model

Assuming a solution with 2.5mm thickness in front of the substrate, one dimensional model has been developed .The solution was segmented into 50 equally spaced segments of width ε along the p-axis as shown in figure 4.1. The segment numbers are 1,2,3,.....i...,50 with concentrations of $C_1,C_2,C_3,...C_i...,C_{50}$ respectively. These concentrations represent the concentration of solute atoms in the solvent. In this case, the solid composition is assumed to be uniform and stoichiometric.

Initially, the solution is perfectly homogeneous and the concentration of solute atoms in the solution is C_E, i.e., $C(p,t=0)=C_E$ for all the positions along the p axis, and to calculate successive concentration profiles after successive time increment τ, one can write $C(p,t)=C(i,n)$ where p=iε and t=nτ (where i is the segment number and n is the number of time cycle).
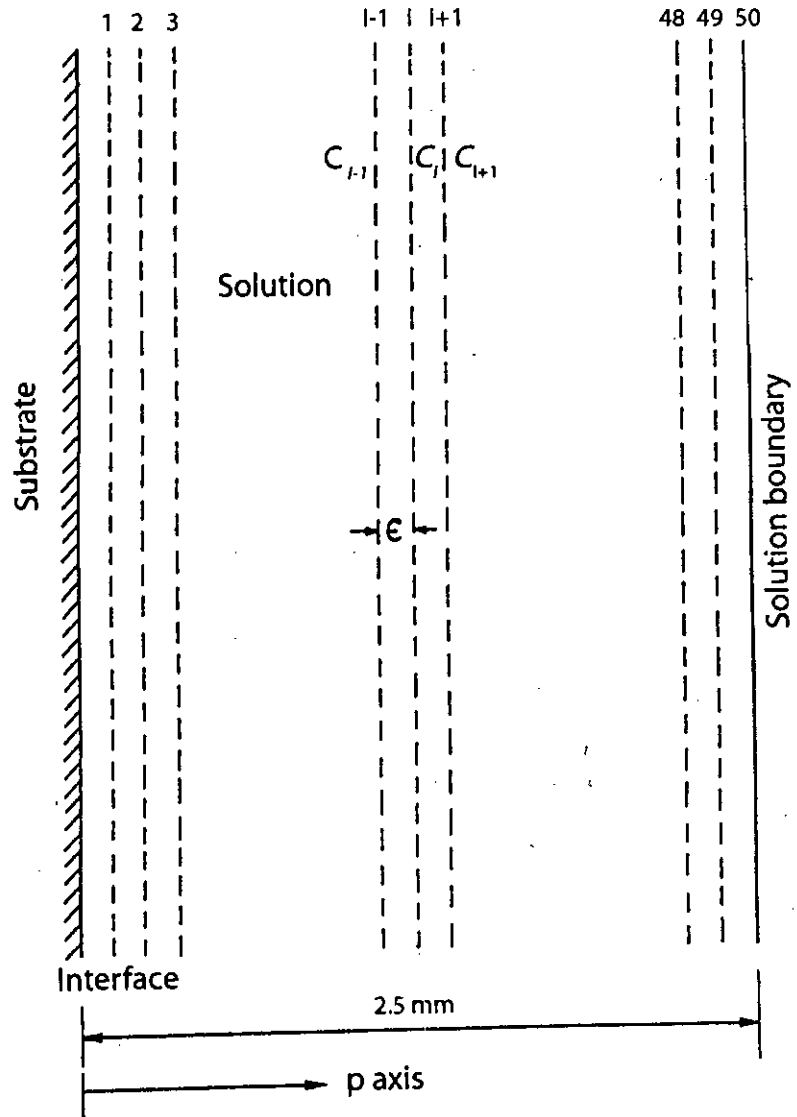
Figure 4.1: Segmented solution in front of growing crystal interface along the axis.

Concentrations C_1 and C_{50} are the first and last segments respectively decided by the boundary conditions. The concentration of solute atoms at the remaining segments during the growth can be calculated by using forward difference in time and the formula for the Laplacian based on a centered difference approximation for the second derivative in p axis (Richard Haberman 1987).

Let the concentration at the points (i+1)ε, iε and (i-1)ε be denoted by $C_u(i+1,n)$, $C_u(i,n)$ and $C_u(i-1,n)$ at time t=nτ respectively. Similarly, let the concentration at the point iε at the time (n+1)τ is denoted by $C_u(i,n+1)$. By applying the Laplacian approximation, we obtain

$$\frac{\partial C_u(p,t)}{\partial p} = \frac{[C_u(i+1,n) - C_u(i-1,n)]}{2\varepsilon} \qquad \text{4.1}$$

$$\frac{\partial^2 C_u(p,t)}{\partial p^2} = \frac{[C_u(i+1,n) - 2C_u(i,n) + C_u(i-1,n)]}{\varepsilon^2} \qquad \text{4.2}$$

$$\frac{\partial C_u(p,t)}{\partial t} = \frac{[C_u(i,n+1) - C_u(i,n)]}{\tau} \qquad \text{4.3}$$

Substituting equation (4.2) and (4.3) in equation (3.10) and rearranging we get one dimensional solute diffusion equation as

$$C_u(i,n+1) = C_u(i,n) + \frac{D_u \tau}{\varepsilon^2}[C_u(i+1,n) - 2C_u(i,n) + C_u(i-1,n)] \qquad \text{4.4}$$

where 'u' is the solute atoms in the solution of ternary system and $\frac{D_u \tau}{\varepsilon^2}$ in the equation 4.4 is called the modulus |M|. |M| should be chosen in such a way as to make |M|≤ ¼ for stability condition (Richard Haberman 1987).

4.2.2 Follow up of phase diagrams

To explain the liquid phase epitaxial growth of ternary compound semiconductors ternary phase diagram is necessary, where ternary composition changes with temperature and is drawn on the basis of diffusion limited experimental thermodynamic data. There are several reports available on experimental and theoretical determination of phase diagrams of ternary III-V compounds and alloys such as InGaAs (Panish 1970; Kuphal 1984; Traeger *et al.*, 1988; Kuphal 1994), InGaP (Stringfellow 1970; Morrison and Bedair 1982; Körber and Benz 1985) and InAsP (Panish and Ilegems 1972; Petzow and Effenberg 1992).

The phase diagram of ternary compound of InGaAs (Kuphal 1994), InGaP (Körber and Benz 1985) and InAsP (Panish and Ilegems 1972) are chosen and presented in figures 4.2, 4.3and 4.4 respectively.

As the phase diagrams give the information in terms atomic fraction of solute atom x_u instead of its absolute concentration C_u, the absolute solute concentration can be expressed in terms of atomic fraction of the components in the liquid phase and solid phase by the following expression (Crossley and Small 1972).

$$C_u = \alpha_L x_u \qquad \text{or} \qquad x_u = \alpha_L^{-1} C_u \qquad\qquad 4.5$$

where C_u and x_u are the absolute concentration and atomic fraction of solute atoms 'u' in the liquid phase respectively and α_L is the constant conversion factor in the liquid phase.
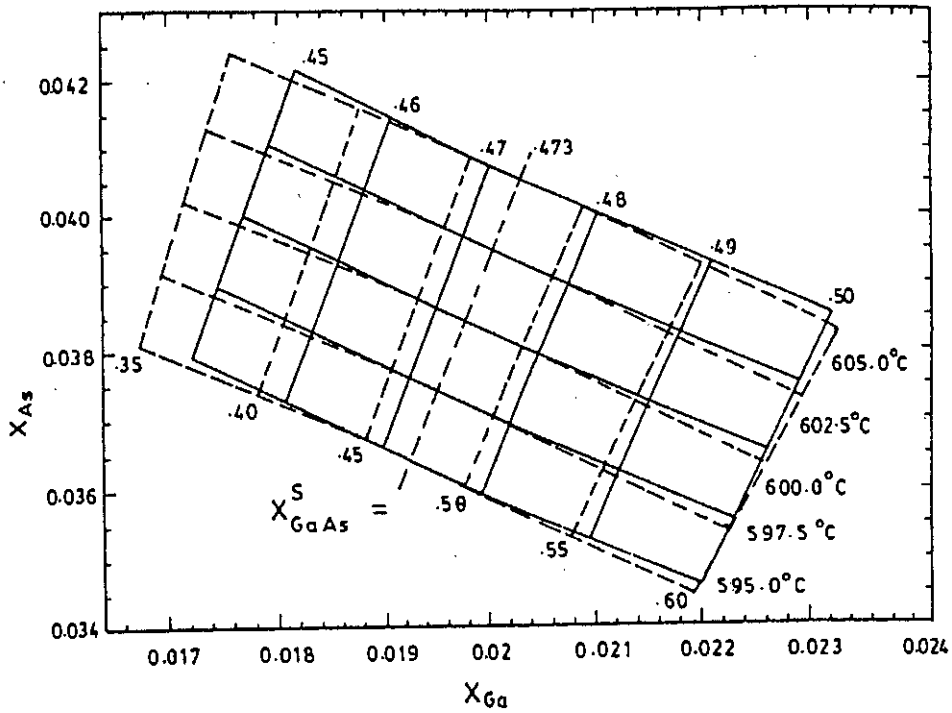
Figure 4.2: Solid-liquid phase diagram of $In_{1-x}Ga_xAs$ near $T=600^0C$. Indicated are isotherms and isoconcentration lines corresponding to the "free" phase diagram (dashed lines) and to the strained diagram (solid lines) for growth on (100)-InP, as well as the line of lattice matching . ($X_{GaAs}=0.473$ at 600^0C) (Kuphal 1994)
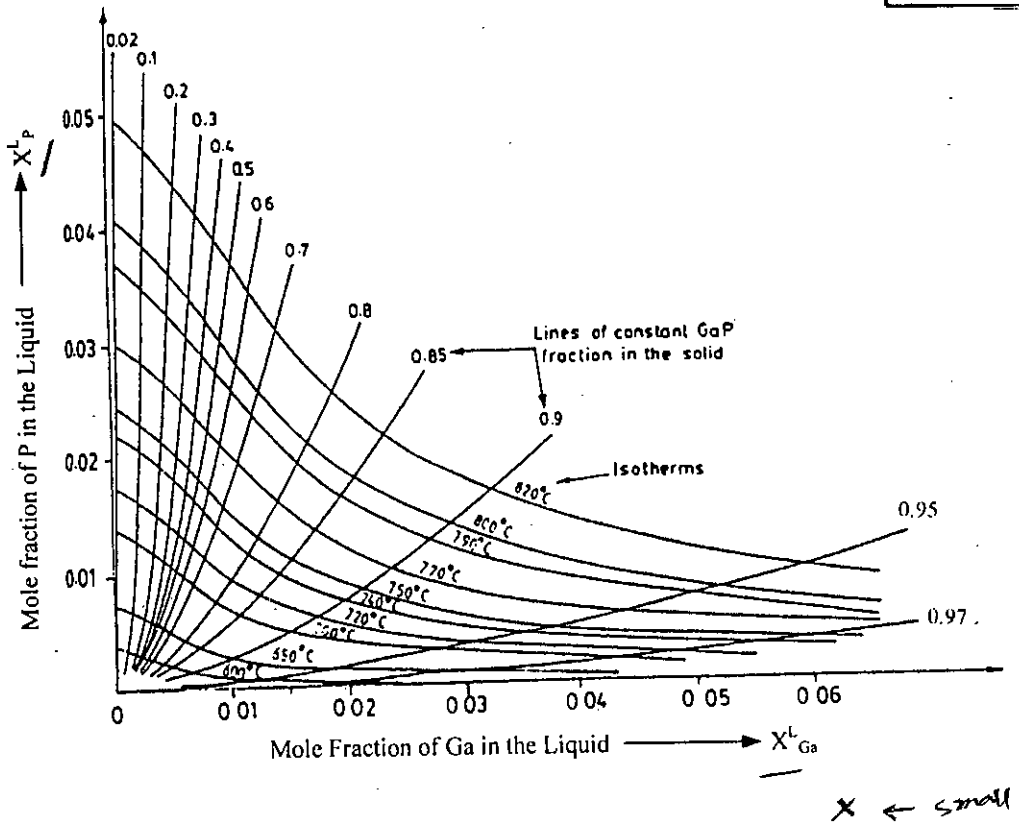
Figure 4.3: Phase diagram of the InGaP system (In-rich side) (Körber and Benz 1985)
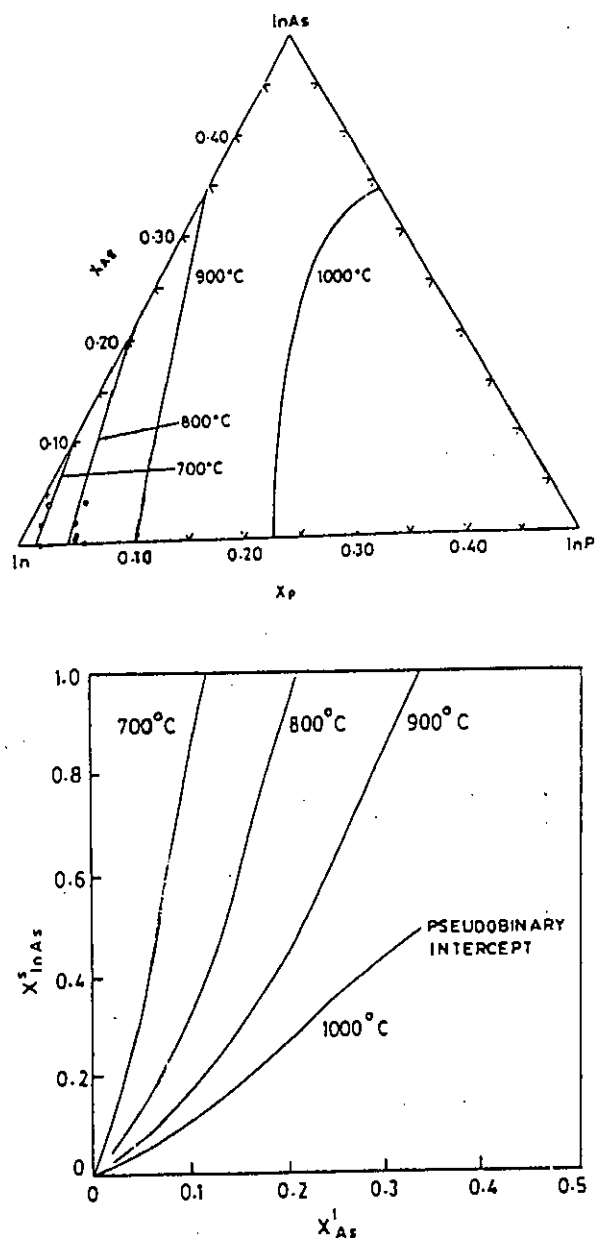
Figure 4.4: Calculated liquidus isotherms (upper graph) and solidus isotherms (lower graph) in the In-rich melt region of the InAsP phase diagrams (Panish and Ilegems 1972).

The atomic fraction of ternary solute atoms in the solid phase as

$$x_V = \alpha_S^{-1} C_V \qquad\qquad 4.6$$

where C_V and x_V are the absolute concentration and atomic fraction of solute atoms 'u' in the solid phase respectively and α_S is the constant conversion factor in the solid phase. The values of the constant conversion factor α_S and α_L have been found out by using the following expressions.

For the liquid phase state

$$\alpha_L = \frac{\text{Density of the liquid phase} \times \text{Avogadros Number (NA)}}{\text{Average molecular weight of the liquid}} \qquad 4.7$$

and for the solid phase state (Kuphal 1994)

$$\alpha_S = \frac{8}{a_l^3} \qquad\qquad 4.8$$

where a_l is the lattice constant of ternary compound($A_{1-x}B_xC$) semiconductors in solid phase which can be expressed as (Olchowik 1994)

$$a_l = f(x_V) = (1-x_V)(a_{AC}) + (x_V)(a_{BC}) \qquad 4.9$$

where a_{AC} and a_{BC} are the two lattice parameters for two binary compounds.

Since the solute atoms are very less compared to the solvent elements in the solution prepared for LPE growth, hence the density and molecular weight of the solution are replaced by the density and molecular weight of the solvent.

4.2.3 Crystallization path

Many researchers (Traeger *et al.*, 1988; Kuphal 1994; Dizaji and Dhanasekaran 1996b) have considered crystallization path during the LPE growth process of III-V ternary compounds.

The schematic phase diagram of a ternary system including crystallization path is shown in figure 4.5, where we have considered a point "a" on the liquidus isotherm corresponding to the initial atomic fraction of x_i^0 and x_j^0 (where i and j are the solute atoms in the solution and i≠j); D_i and D_j are the diffusion coefficient of the dissolved components of i and j respectively at the temperature T. When the temperature of the ternary growth system is cooled to the temperature T-ΔT, then the following two extreme cases can be considered: (i) if D_i>>D_j, then the solute atomic fraction (x_i^0) remains constant (i.e. initial or equilibrium atomic fraction x_i^0) up to point "b" on the liquidus isotherm T-ΔT and (ii) if D_j>>D_i, the solute atomic fraction (x_j^0) remains constant (i.e. initial or equilibrium atomic fraction of x_j^0) up to a point "c" on the liquidus isotherm T-ΔT. The solute atomic fraction shifts on a rectilinear path from the liquidus isotherm corresponding to temperature T to the liquidus isotherm corresponding to temperature T-ΔT at all allowed points between "b" and "c" on the liquidus isotherm of T-ΔT depending upon the composition of the solid phase and the ratio of the diffusion coefficients of solute atoms (D_i/D_j) say crystallization line is "ad" as shown in figure 4.5, and the point "d" lies on the liquidus isotherm of T-ΔT. For isothermal growth from a sufficient large solution, points "a" and "d" are time

independent, i.e. the solid composition is constant during growth, but it depends linearly on ΔT. So, the change in initial solute atomic fraction x_i^0 at the interface due to the small decrease in temperature ΔT, the crystallization (solidification) path can be described by the following linear expression

$$\Delta x_i = \Delta x_i^* - \beta \Delta x_j \qquad\qquad 4.10$$

where $\Delta x_i^* = x_i^0 - x_i^*$, x_i^* is the atomic fraction of solute i at the interface at $T-\Delta T$ with the condition $D_j >> D_i$, x_i^0 is the initial atomic fraction of solute i at the equilibrium temperature T and the coefficient β (which depends on temperature and atomic fraction of solute atoms i and j) can be expressed (Traeger at al 1988) as a slope at the point "d" where the rectilinear path (crystallization path) intersects on the liquidus isotherm $T-\Delta T$ in the x_i versus x_j phase diagram.

$$\beta = -\frac{\partial x_i}{\partial x_j} = \left(\frac{\partial T}{\partial x_j}\right) \times \left(\frac{\partial x_i}{\partial T}\right) \qquad\qquad 4.11$$

the flux of a solute atoms in a ternary solution given at the liquid-solid interface is given by (Dutartre 1983)

$$F_u = \frac{1}{m_u}\left(\frac{D_u}{\pi}\right)^{1/2}\left(\Delta T t^{-1/2} + 2\alpha t^{1/2}\right) \qquad\qquad 4.12$$

where F_u is the flux of solute atoms "u", m_u is the slop of the liquidus defined as $m_u = (\partial T / \partial x_u)$ at the point "d" where the crystallization path intersects the liquidus isotherm $T-\Delta T$, α is the cooling rate $(-\partial T/\partial t)$. ΔT is the initial supercooling and D_u is the diffusion coefficient of solute atoms.
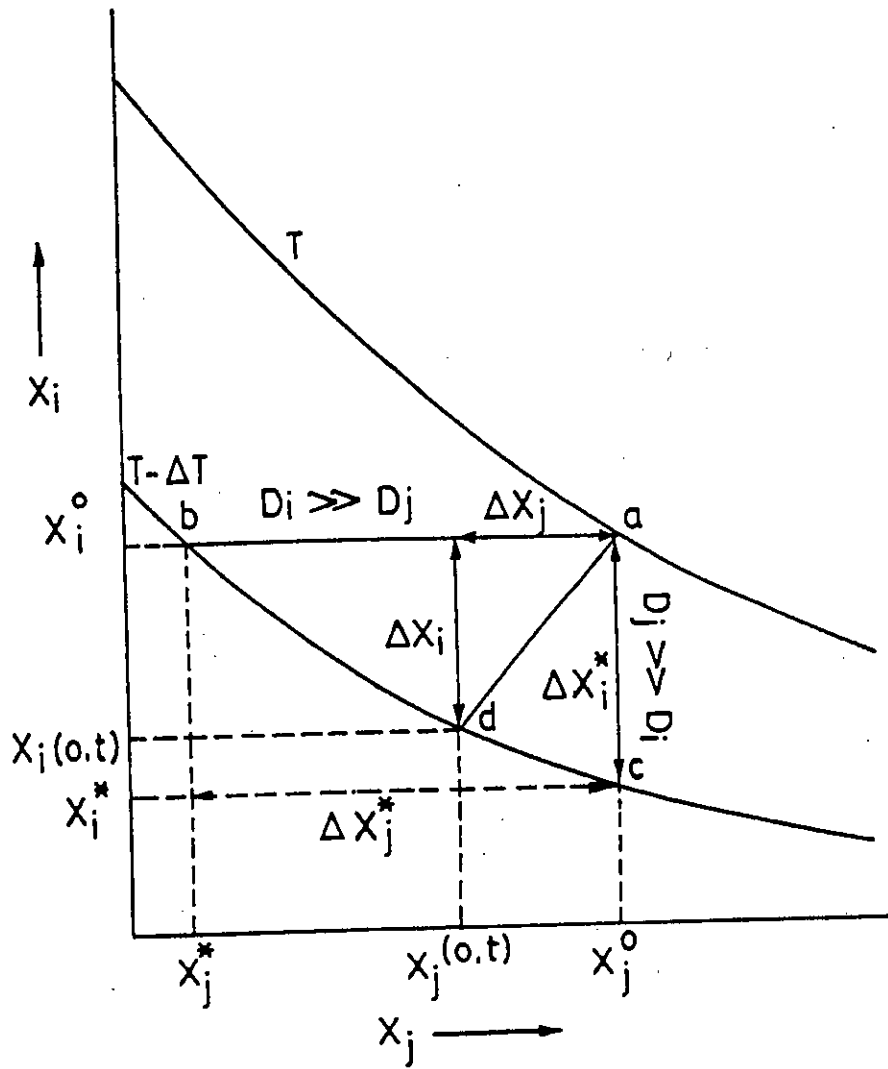
Figure 4.5: Schematic phase diagram of a ternary system.

Let us consider the ternary III-III-V systems. As an example $In_{1-x}Ga_xAs$ with the reference to figure 4.5 (where i=As and j=Ga), the equation (4.10) becomes

$$\Delta x_{As} = \Delta x_{As}^* - \beta \Delta x_{Ga} \qquad 4.13$$

where $\Delta x_{As}^* = x_{As}^0 - x_{As}^*$, x_{As}^* is the atomic fraction of arsenic (As) at the interface at temperature T-ΔT with the condition $D_{Ga} >> D_{As}$, x_{As}^0 is the initial value of the As atomic fraction at the equilibrium temperature T_E.

Applying the equation (4.12) to ternary $In_{1-x}Ga_xAs$ system, the fluxes of the solute atoms As and Ga are given by

$$F_{As} = \frac{1}{m_{As}} \left(\frac{D_{As}}{\pi} \right)^{1/2} \left(\Delta T t^{-1/2} + 2\alpha t^{1/2} \right) \qquad 4.14$$

$$F_{Ga} = \frac{1}{m_{Ga}} \left(\frac{D_{Ga}}{\pi} \right)^{1/2} \left(\Delta T t^{-1/2} + 2\alpha t^{1/2} \right) \qquad 4.15$$

Since the mole fraction of solute atoms in the solid phase X_V (v = GaAs or InAs) is much larger than the atomic fraction of the solute atoms in liquid phase x_u (u = Ga or As), the flux of each species (F_{As}, F_{Ga}) must be proportional to its constituent solid mole fraction at any time and thus,

$$\frac{F_{Ga}}{F_{As}} = X_{GaAs} \qquad 4.16$$

Substituting equation (4.14) and (4.15) in equation (4.16) we get,

$$X_{GaAs} = \frac{m_{As}}{m_{Ga}} \left(\frac{D_{Ga}}{D_{As}} \right)^{1/2} \qquad 4.17$$

or, $\qquad X_{GaAs} = \dfrac{\Delta x_{Ga}}{\Delta x_{As}}\left(\dfrac{D_{Ga}}{D_{As}}\right)^{1/2}$

or, $\qquad \Delta x_{Ga} = \Delta X_{GaAs}\Delta x_{As}\left(\dfrac{D_{As}}{D_{Ga}}\right)^{1/2}$ $\qquad\qquad$ 4.18

where $m_{As}=(\Delta T/\Delta x_{As})$ and $m_{Ga}=(\Delta T/\Delta x_{Ga})$ are the slope of the liquidus at the point

where the crystallization path intersects the liquidus isotherm T-ΔT.

Substituting Δx_{As} from the equation (4.13) in equation (4.18) and the value

of $\Delta x_{Ga}=[x_{Ga}]_T-[x_{Ga}]_{T-\Delta T}$, we obtain by rearranging

$$[x_{Ga}]_{T-\Delta T} = [x_{Ga}]_T - \frac{X_{GaAs}\left(\dfrac{D_{As}}{D_{Ga}}\right)^{1/2}\Delta x_{As}^{\bullet}}{1+\beta X_{GaAs}\left(\dfrac{D_{As}}{D_{Ga}}\right)^{1/2}} \qquad\qquad 4.19$$

Using the above equation (4.19) along with an expression developed for

solid mole fraction, X_{GaAs} and by applying the values of diffusion coefficients of

the solute atoms, the equilibrium atomic fraction of the solute atoms for successive

time increment can be calculated at the growing interface.

Similarly, for the ternary III-V-V systems as an example $InAs_xP_{1-x}$ with the

reference to figure 4.5 (where i=As and j=P), we can write the equation (4.10) as

$$\Delta x_P = \Delta x_P^{\bullet} - \beta^{-1}\Delta x_{As} \qquad\qquad 4.20$$

where $\Delta x_P^{\bullet} = x_P^0 - x_P^{\bullet}$, $x_P^{\bullet}$ is the atomic fraction of phosphorus (P) at the interface at

temperature T-ΔT with the condition $D_P >> D_{As}$, x_P^0 is the initial value of atomic

fraction P at the equilibrium temperature T_E.

Applying the equation (4.12) to ternary $InAs_xP_{1-x}$, the system, while the flux of As is given by equation (4.14), the flux of the solute atoms P is given by

$$F_P = \frac{1}{m_P}\left(\frac{D_P}{\pi}\right)^{1/2}\left(\Delta T t^{-1/2} + 2\alpha t^{1/2}\right) \qquad 4.21$$

From the concept of flux of each species which must be proportional to its constituent solid mole fraction at any time as

$$\frac{F_{As}}{F_{In}} = X_{InAs} \qquad 4.22$$

$$\frac{F_P}{F_{In}} = 1 - X_{InAs} \qquad 4.23$$

where X_{InAs} is the mole fraction of solute atoms in the solid phase. Dividing equation (4.22) by equation (4.23) we get

$$\frac{X_{InAs}}{1 - X_{InAs}} = \frac{F_{As}}{F_P} \qquad 4.24$$

Substituting equation (4.14) and (4.21) in equation (4.24) we get

$$\frac{X_{InAs}}{1 - X_{InAs}} = \frac{m_P}{m_{As}}\left(\frac{D_{As}}{D_P}\right)^{1/2} \qquad 4.25$$

or, $$\frac{X_{InAs}}{1 - X_{InAs}} = \frac{\Delta x_{As}}{\Delta x_P}\left(\frac{D_{As}}{D_P}\right)^{1/2}$$

or, $$\Delta x_{As} = \frac{X_{InAs}}{1 - X_{InAs}}\Delta x_P\left(\frac{D_P}{D_{As}}\right)^{1/2} \qquad 4.26$$

where $m_{As} = (\Delta T/\Delta x_{As})$ and $m_P = (\Delta T/\Delta x_P)$ are the slope of the liquidus at the point where the crystallization path intersects the liquidus isotherm $T - \Delta T$.

Substituting Δx_P from the equation (4.20) in equation (4.26) and the value

of $\Delta x_{AS}=[x_{As}]_T-[x_{As}]_{T-\Delta T}$, we obtain by rearranging

$$[x_{As}]_{T-\Delta T} = [x_{As}]_T - \frac{\dfrac{X_{InAs}}{1-X_{InAs}}\left(\dfrac{D_P}{D_{As}}\right)^{1/2}\Delta x_P^*}{1+\beta^{-1}\dfrac{X_{InAs}}{1-X_{InAs}}\left(\dfrac{D_P}{D_{As}}\right)^{1/2}} \qquad 4.27$$

Using the above equation (4.27), along with an expression developed for

solid mole fraction, X_{InAs}, and by applying the values of diffusion coefficients of

the solute atoms, the equilibrium atomic fraction of the solute atoms can be

calculated at the growing interface.

4.3   Calculation method of ternary system

To construct concentration profiles and concentration profile surface of

solute atoms 'u' during the LPE growth process, the solution of 2.5mm thickness

initially assumed to be composition of uniform melt (perfectly homogeneous) in

the solution for all positions (p,q),i.e. $x_u(p,q,t)=x_u^0$ when time T=0. One can choose

the initial temperature of the melt and the atomic fraction of solute atoms on the

basis of experimental values from the reported literature and to find out the other

solute atomic fraction, the theoretical phase diagram (respective ternary system)

may be used at that temperature. These initial atomic fractions of the solute atoms

are fed into the meshes corresponding to the 50×50 positions in space.

Applying the concentration data with appropriate boundary conditions, we

can simulate the concentration profiles and concentration contours of solute atoms

in front of growing crystal interface along the distance perpendicular to the

substrate. Also the average growth rate, the layer thickness along the distance perpendicular to the substrate, dimensionless concentration parameter as a function of time and the solid composition as a function of temperature and time can be computed. The temperature contours in the melt have also been constructed.

4.3.1 Boundary condition

The solid composition of the growing layer from an N component liquid is a function of the atomic fraction of (N-2) components and the temperature. We can write in the $In_{1-x}Ga_xAs$ LPE case, as

$$X_{GaAs} = f_1(x_{Ga}, T) \qquad\qquad 4.28$$

. The equilibrium atomic fraction of a component in the liquid can be written as a function of atomic fraction of (N-2) other components and the temperature. Thus, we can write as

$$x_{Ga}^E = f_2(x_{As}, T) \qquad\qquad 4.29$$

Since the first segment is always assumed to be saturated at a given temperature T, then the atomic fraction of x_{Ga} between nth and (n+1)th time increments (where the temperature is reduced by ΔT and the solution is supersaturated) we have

$$(x_{Ga})_{0,n+1} = f_3\left[(x_{As})_{0,n+1}, \Delta T\right] \qquad\qquad 4.30$$

For satisfying the equations (4.28) to (4.30), the conservation of each component also be satisfied.

4.3.2 Growth rate in ternary system

The average growth rate of ternary compound system can be calculated by the following equation for finite difference (Crossley and Small 1972) at the end of each step in the computation of the equation (4.2) as

$$R = \frac{\alpha_L D_u}{\varepsilon} \left[\frac{x_u(1,n) - x_u(0,n+1)}{0.5\alpha_S X_V - \alpha_L x_u(0,n+1)} \right] \qquad 4.31$$

where $x_u(0,n+1)$ and $x_u(1,n)$ are the atomic fraction of solute atoms at the interface of $(n+1)$th time and first layer of nth time respectively. α_L and α_S are the conversion factors in liquid solid phase respectively. X_V is the solid mole fraction in ternary system. The average thickness of the growth crystal at any time is obtained by the summation of the growth rate as

$$d = \sum_{n+1} R\tau = \sum_{n+1} \frac{\alpha_L D_u \tau}{\varepsilon} \left[\frac{x_u(1,n) - x_u(0,n+1)}{0.5\alpha_S X_V - \alpha_L x_u(0,n+1)} \right] \qquad 4.32$$

An equation for layer thickness of the grown crystal at any time can be found out by the following expression for finite difference at the end of each time step in the computation of the equation (4.4) as

$$d(j) = \sum_{n+1} R(j)\tau = \sum_{n+1} \frac{\alpha_L D_u \tau}{\varepsilon} \left[\frac{x_u(1,j,n) - x_u(0,j,n+1)}{0.5\alpha_S X_V - \alpha_L x_u(0,j,n+1)} \right] \qquad 4.33$$

where $0 \leq j \leq 25$; $x_u(0,j,n+1)$ and $x_u(1,j,n)$ are the atomic fraction of solute atoms at the interface and first layer (perpendicular direction to the substrate) respectively.

4.3.3 Dimensionless concentration parameter

The dimensionless parameter is defined (Wilcox 1982) as

$$L_u = \frac{x_u^0 - x_u}{x_u^0 - x_u^E} \qquad\qquad 4.34$$

where x_u^0, x_u^E and x_u are the initial atomic fraction, atomic fraction at the crystal surface (which is a function of time or growth temperature), and atomic fraction at any position during the growth process respectively. This parameter goes from one to zero. One can use a combination form of the above equation (4.34) as an example of ternary InGaAs system for calculating the dimensionless concentration parameter as

$$L_C = \frac{(x_{Ga}^0 + x_{As}^0) - (x_{Ga} + x_{As})}{(x_{Ga}^0 + x_{As}^0) - (x_{Ga}^E + x_{As}^E)} \qquad\qquad 4.35$$

Chapter V

Results and Discussions

Results and Discussion

5.1 Introduction

Using numerical simulation methods, one dimensional models have been constructed to calculate the successive concentration profiles, layer thickness along the distance perpendicular to the substrate, dimensionless concentration parameter of solute atoms in front of growing crystal interface by Liquid Phase Epitaxial growth for $In_{1-x}Ga_xAs$, $In_{1-x}Ga_xP$ and $InAs_xP_{1-x}$ ternaries and the results are discussed in the following sections.

5.2 Indium Gallium Phosphide ($In_{1-x}Ga_xP$)

According to the experimental report (Mariette et al 1981), the initial or equilibrium atomic fraction of Gallium (Ga) atoms in the case of InGaP has been considered as 0.01198 at the equilibrium temperature T_E=1103K. The coefficient β and the atomic fraction Δx_p^* have been calculated from the isotherm liquidus curve (Körber and Benz 1985). The temperature dependent diffusion coefficient of Ga and P in In-rich melt have been considered D_{Ga}=0.83 exp(-9137/T) cm^2/sec and D_P=7.23x10^{-3}exp(-3819/T) cm^2/sec respectively from the literature (Dobosz and Zytkiewicz 1991).

An expression has been developed for the equilibrium atomic fraction of P, x_P, as a function of atomic fraction of Ga, x_{Ga} and the temperature T by using the InGaP ternary phase diagram (Körber and Benz 1985) as

$$x_P = \exp(11.00029 - 1.500011 \times 10^4/T - 1.001486 \times 10^{-4}T) \times$$

$$\exp(6.998186 \times 10^{-4}/x_{Ga} - 48.976666 x_{Ga}) \qquad 5.1$$

Equitation for solid mole fraction of Ga in solid phase X_{GaP} has been developed by using the phase diagram (Panish and Ilegems 1972) as a function of atomic fraction of Ga, x_{Ga} in liquid phase and the temperature T as

$$X_{GaP} = \exp(25 - 2.599989 \times 10^4/T - 3.181997 \times 10^{-2}T) \times$$

$$\exp(30.63267 - 2.07398 \times 10^{-3}/x_{Ga} - 2.10009 \times 10^2 x_{Ga}) \qquad 5.2$$

Flux for P and the same process as for InGaAs to get equation 4.19 is also used here. And this leads to the following expression of atomic fraction of Ga, x_{Ga} for the next successive time increment in the InGaP LPE growth

$$[x_{Ga}]_{T-\Delta T} = [x_{Ga}]_T - \frac{X_{GaP}\left(\dfrac{D_P}{D_{Ga}}\right)^{1/2} \Delta x_P^{\bullet}}{1 + \beta X_{GaP}\left(\dfrac{D_P}{D_{Ga}}\right)^{1/2}} \qquad 5.3$$

·Now using the above three equations 5.1 to 5.3 with 4.4 we can construct the atomic fraction profiles of solute (Ga and P) atoms inside the melt in front of growing crystal interface as the growth proceeds.

5.2.1 Results and discussion

Figure 5.1 shows the mole fraction of solute atoms in solid phase as a function of temperature at cooling rates of 0.25K/min, 0.5K/min and 1.0K/min. It

is observed that no change in the shape of the curve is found with change in cooling rates. But the solid mole fractions as a function of thickness of the grown layers are very much affected by the cooling rate as shown in figure 5.2.

Figure 5.3 represents the calculated average thickness of the layers as a function of temperature at four different cooling rates (0.25K/min, 0.33K/min, 0.5K/min and 1.0K/min). It is found that for a given ending temperature (T_{END}=1013K), higher the cooling rate, lower is the thickness of the grown InGaP layers. This may be due to shorter time available for the growth.

Figure 5.4 shows the thickness of the grown layers as a function of time at different cooling rates (0.25K/min, 0.33K/min, 0.5K/min and 1.0K/min). It may be observed that, for any growth time, the solution that is more rapidly cooled produce more rapid growth. At longer duration of the experiment we expect the growth at lower cooling rate to continue. Growth at higher cooling rates is expected to stop due to the rapid consumption of solute atoms, which may produce imperfections in crystal structure.

Figures 5.5 and 5.6 are the one dimensional atomic fraction profiles of Ga and P atoms in front of growing crystal interface at different growth temperatures and a cooling rate of 0.5k/min. Initially the melt contained 0.01198 and 0.3924 atomic fraction of Ga and P atoms respectively in a In-rich melt. The concentration profiles of both Ga and P show that relation between change in solute and change of distance from substrate is more linear in case of ternary alloys cooled to lower temperatures.
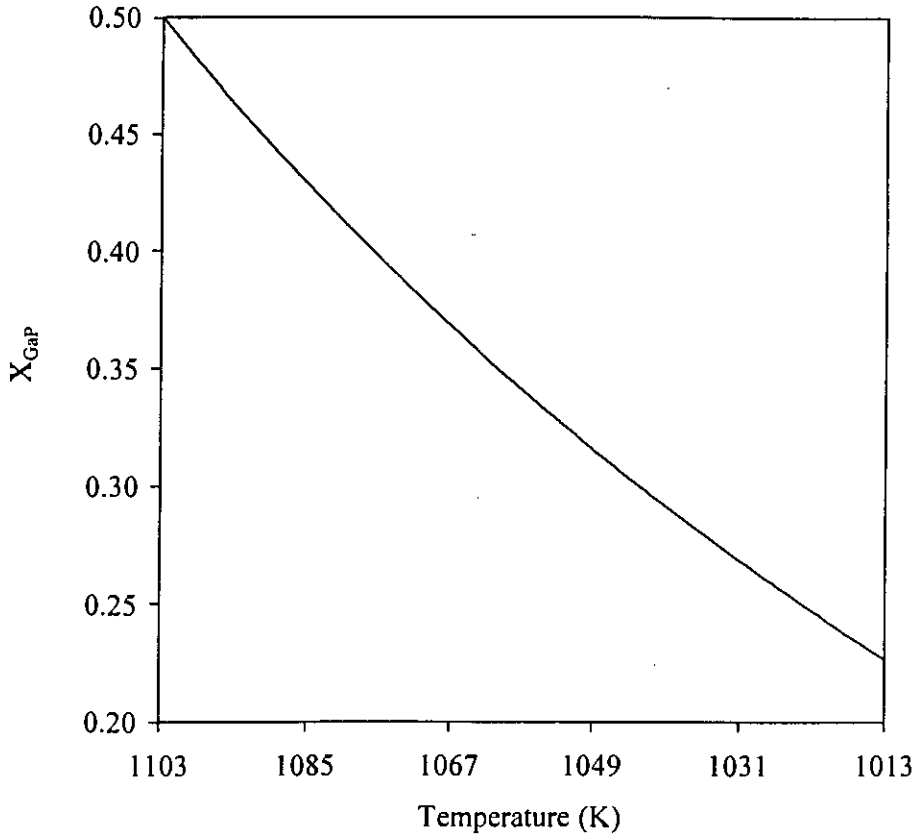
Figure 5.1: Calculated values of GaP solid mole fraction in the InGaP alloy as a function of temperature for $T_E=1103K$ and cooling rates of 1.0K/min, 0.5K/min and 0.25K/min.
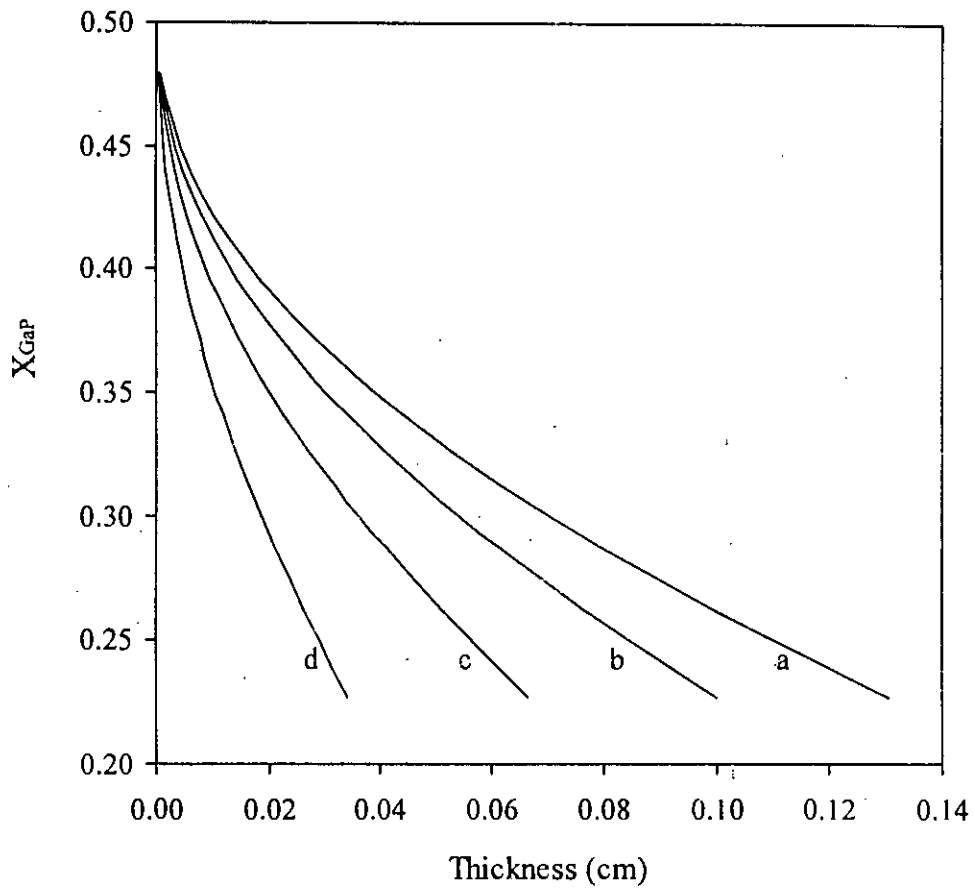
Figure 5.2: Simulated values of GaP solid mole fraction in InGaP alloy as a function of thickness of the grown layer for different cooling rates of: a) 0.25K/min, b) 0.33K/min, c) 0.5K/min and d) 1.0 K/min for T_E=1103K with the ending point of each curve corresponding to T_{END}=1013K.
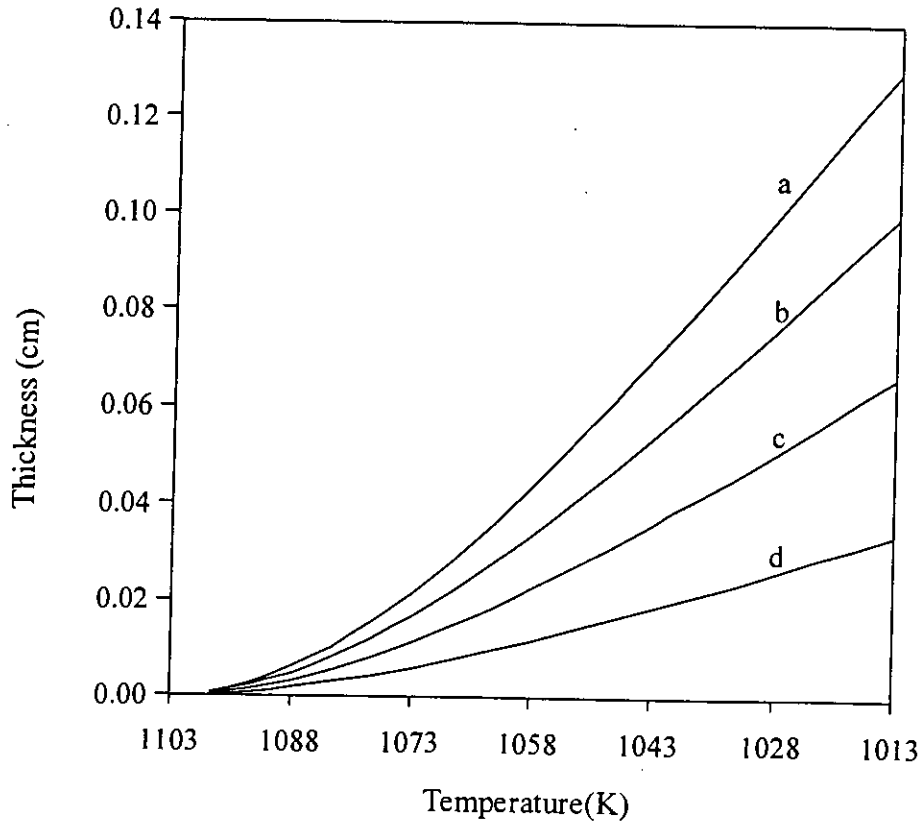
Figure 5.3: Thickness grown as function of temperature for various cooling rates of: a) 0.25K/min, b) 0.33K/min, c) 0.5K/min and d) 1.0 K/min for T_E=1103K with the ending point of each curve corresponding to T_{END}=1013K.
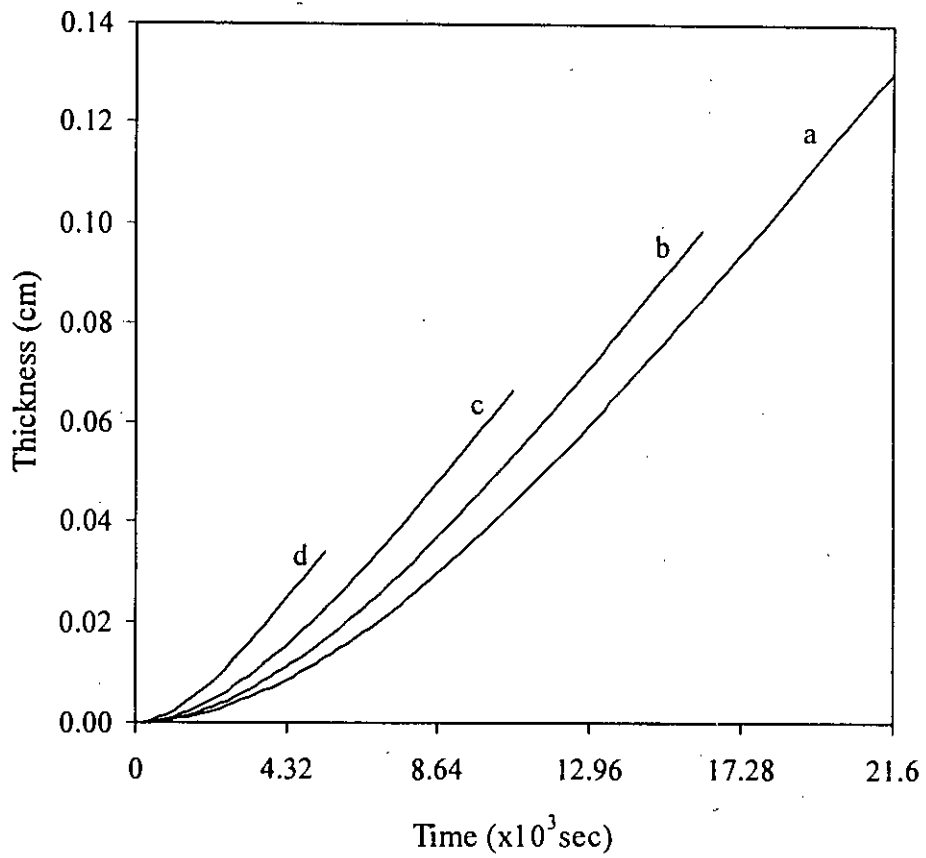
Figure 5.4: Thickness grown as function of time for different cooling rates of: a) 0.25K/min, b) 0.33K/min, c) 0.5K/min and d) 1.0 K/min for T_E=1103K with the ending point of each curve corresponding to T_{END}=1013K.
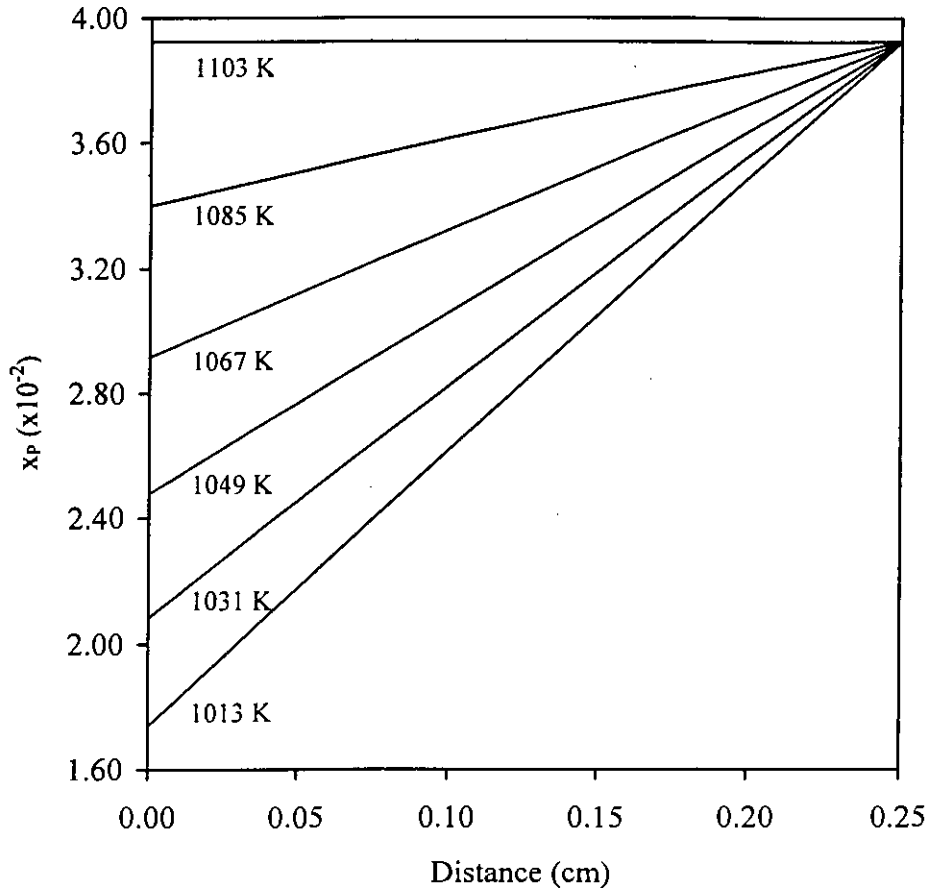
Figure 5.5: Atomic fraction profile of P atoms in In-rich melts at different growth temperatures for the given cooling rate of 0.5K/min and equilibrium temperature T_E=1103K for distances measured from solid liquid interface.
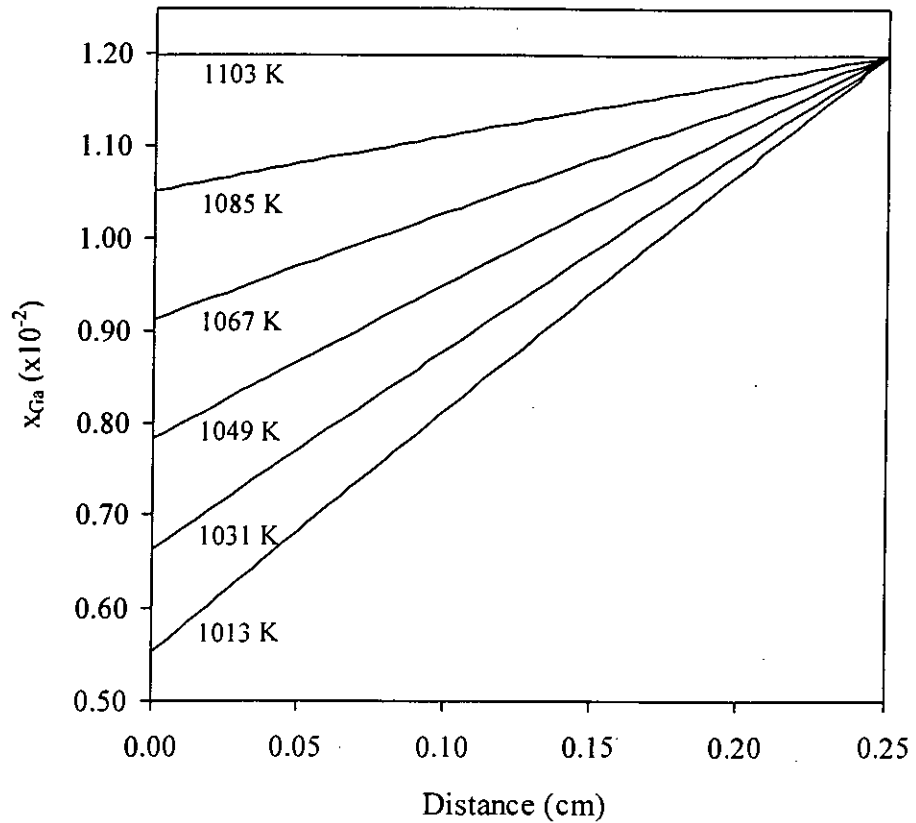
Figure 5.6: Atomic fraction profile of Ga atoms in In-rich solution at different growth temperatures for the given cooling rate of 0.5K/min and equilibrium temperature T_E=1103K and for distances measured from solid liquid interface.

Figure 5.7: Dimensionless concentration profile of Ga in front of the crystal growing interface at different growth time for cooling rate 0.5K/min and T_E=1103K
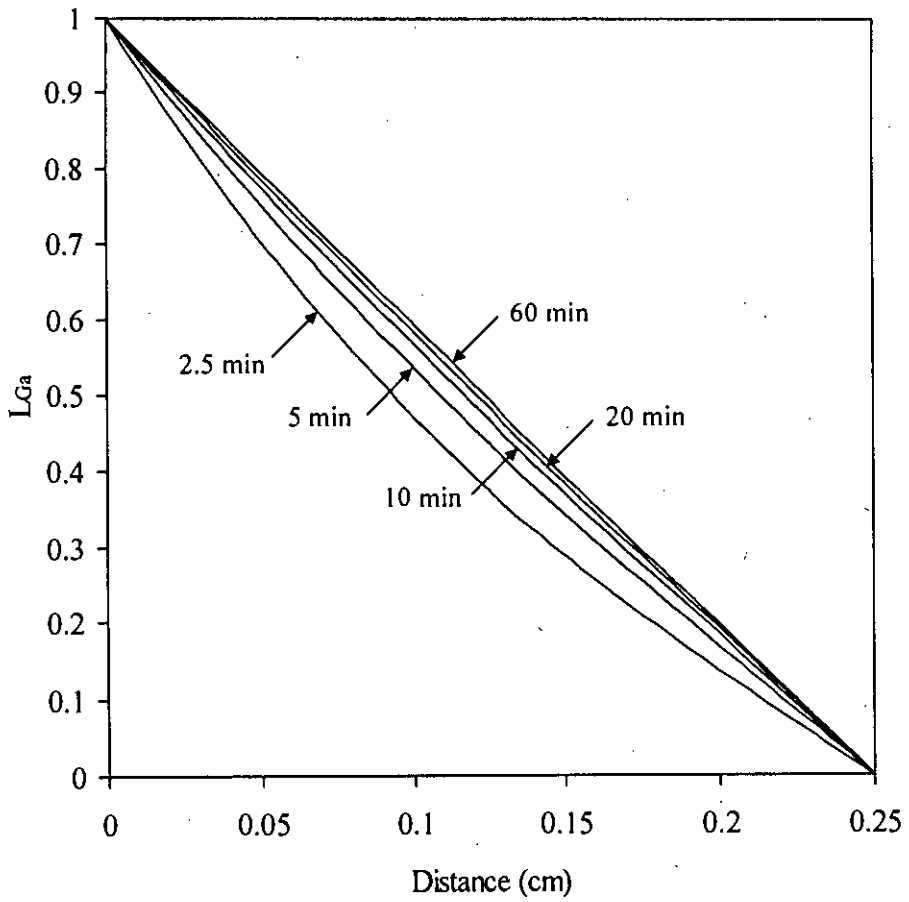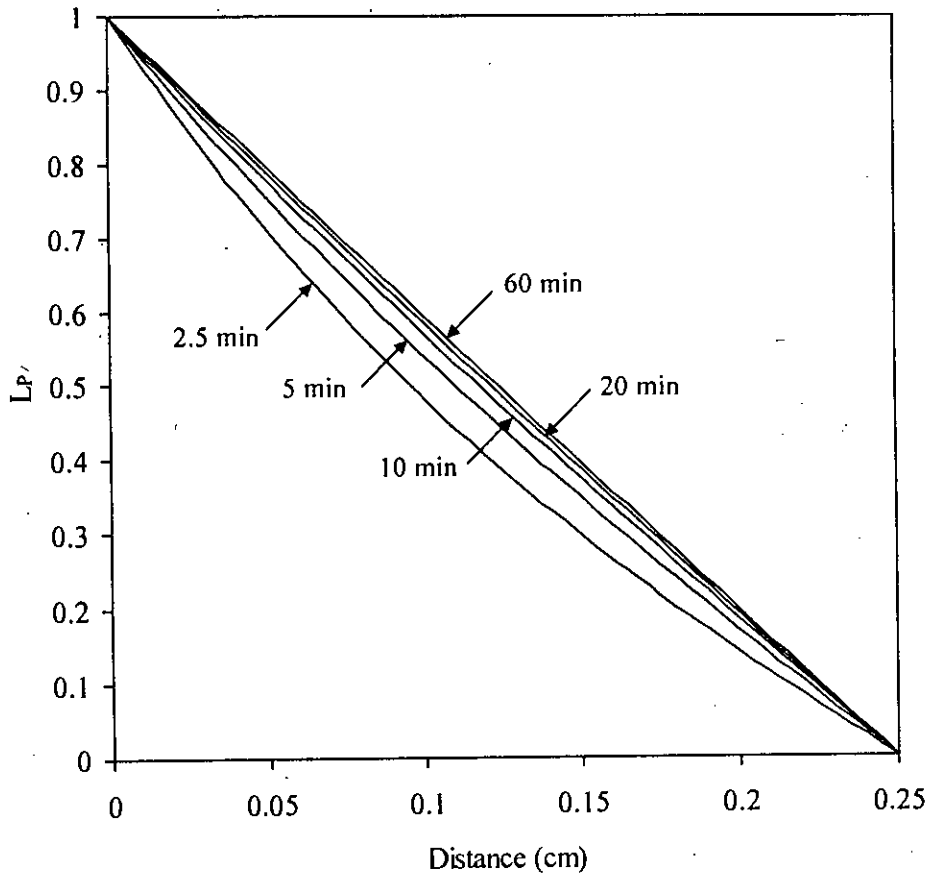
Figure 5.8: Dimensionless concentration profile of P in front of the crystal growing interface at different growth time for cooling rate 0.5K/min and T_E=1103K.
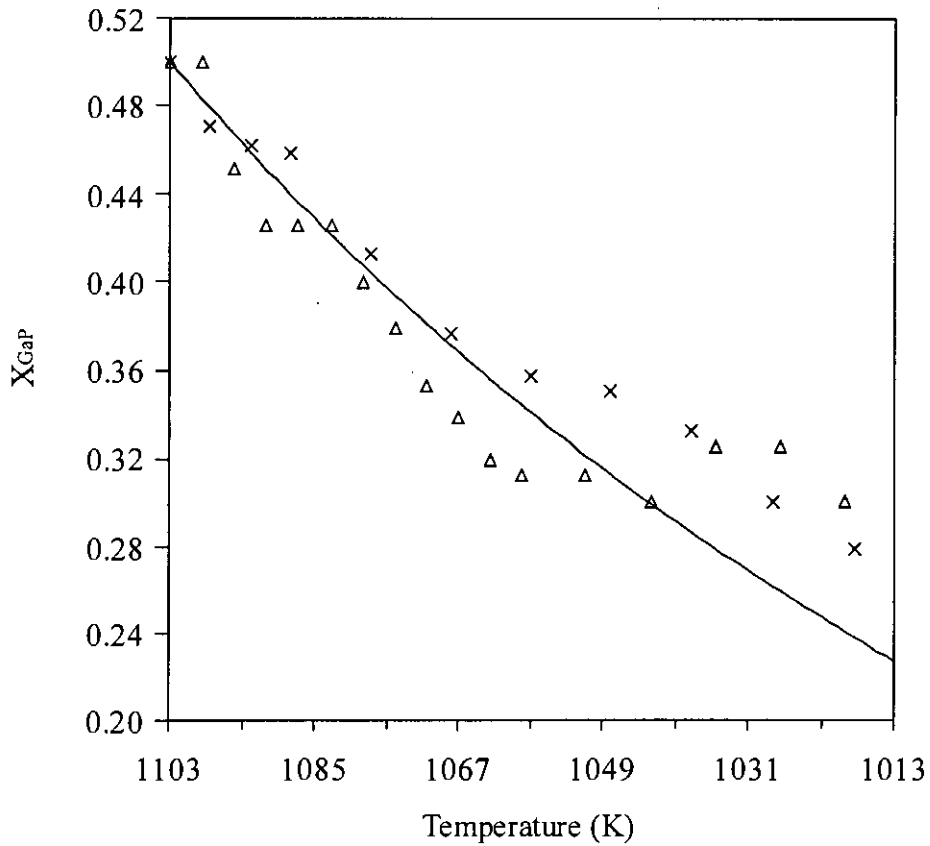
Figure 5.9: Comparison between our theoretical results and experimentally reported values (for T_E=1103K and cooling rate of 0.33K/min). (Δ, x) experimental points (Mariette et al 1981), and (—) the present work.

Figures 5.7 and 5.8 show the dimensionless concentration profile for Ga and P atoms in the melt at different growth time with cooling rate of 0.5K/min. It is found that the curves for lower growth times are more distinguishable for Ga than P. This may be due to faster saturation of Ga atoms in the melt at lower growth time.

The result obtained from present theoretical model has been compared with the reported (Mariette et al 1981) results under same experimental conditions are shown in figure 5.9. Good agreement is found between our theoretical findings and the reported values.

5.3 Indium Gallium Arsenide (In$_{1-x}$Ga$_x$As)

At the equilibrium temperature T_E=871.2K, atomic fraction of Ga atoms in the liquid phase has been found out as 0.0196 on the basis of reported literature (Kuphal 1994). The coefficient β (which depends on temperature and atomic fraction of solute atoms) and the atomic fraction Δx_{As}^* (which depends on cooling rate, successive time increment and atomic fraction of solute atoms) have been calculated from the isotherm liquidus curve of InGaAs (Kuphal 1991). The diffusion coefficient of Ga and As in In-rich melt have been considered D_{As}=8.9×10^{-5} cm^2/sec and D_{Ga}=3.7×10^{-5} cm^2/sec from the literature (Traeger et al 1988).

In the liquid phase, the equilibrium atomic fraction of As, x^E_{As}, for InGaAs system has been developed as a function of atomic fraction of Ga, x_{Ga}, and the temperature T using the InGaAs ternary phase diagram (kuphal 1994) as

$$x^E_{As}= \exp(43.75616-2.498563\times10^4/T-2.005283\times10^{-2}T)\times$$

$$\exp(- 4.830697\times10^{-3}/x_{Ga}-32.55606x_{Ga}) \qquad\qquad 5.4$$

The following expression for the mole fraction of GaAs in the solid phase X_{GaAs}, has been developed by using the phase diagram (Traeger et al 1988) as a function of atomic fraction of Ga, x_{Ga}, and the temperature T

$$X_{GaAs}=\exp(32.\ 72766-8.778193\times10^3/T-2.315285\times10^{-2}T)\times$$

$$\exp(-5.110814\times10^{-2}/x_{Ga}-31.83753x_{Ga}) \qquad\qquad 5.5$$

The equilibrium atomic fraction of Ga, x_{Ga} in liquid phase at the next lower temperature can be determined using equation 4.19. With equations 4.4, 4.19, 5.4 and 5.5, the concentration profiles of solute species inside the solution in front of the growing crystal interface have been constructed for one-dimensional model of the ternary.

5.3.1 Results and discussion

Figure 5.10 and 5.11 shows one dimensional calculated atomic fraction profile of Ga and As atoms inside the InGaAs solution for the cooling rate of 0.5K/min for various growth temperatures. It is observed that the change of solute fraction of Ga and As atoms with distance from the substrate are higher for the ternary cooled at lower temperatures.

Figures 5.12 and 5.13 show the dimensionless concentration parameters for Ga and As in the melt at different growth time with a cooling rate of 1K/min respectively. It is seen that the curves for lower growth time are more distinguishable from each other in the case of gallium than in the case of arsenic.

This may be attributed to the faster saturation of Ga atoms in the melt at lower growth time.

Figure 5.14 gives the solid mole fraction of GaAs as a function of temperature with different cooling rates. No difference was observed when the same parameter was determined for any one of the four cooling rates (0.25K/min, 0.33K/min, 0.50K/min and 1K/min). The solid mole fractions as a function of thickness of the grown layers at four different cooling rates (0.25K/min, 0.5K/min 0.75K/min and 1K/min) are represented in figure 5.15. It is seen that the mole fraction of the growing solid is very much affected by the cooling rate. For a particular layer thickness, the solid composition of GaAs is greater for lower cooling rates than for the higher ones.

Figure 5.16 displays the results of the thickness of the grown layers as a function of temperature at different cooling rates (0.25K/min, 0.5K/min 0.75K/min and 1K/min). It may be observed that, for a certain level of growth temperature (T_{END}=820K), the thickness of the grown layer is more for lower cooling rate than that of higher cooling rate. This may be due to the fact that longer time is available for the growth of lower cooling rate and shorter time is available for higher cooling rate for the growth of the ternary compound. The average layer thickness of the grown InGaAs is calculated as a function of time at four different cooling rates as shown in figure 5.17. The ending point of each curve represents the end temperature T_{END}=820K. It is seen that rapid cooling leads to the rapid growth of crystal for any growth time.
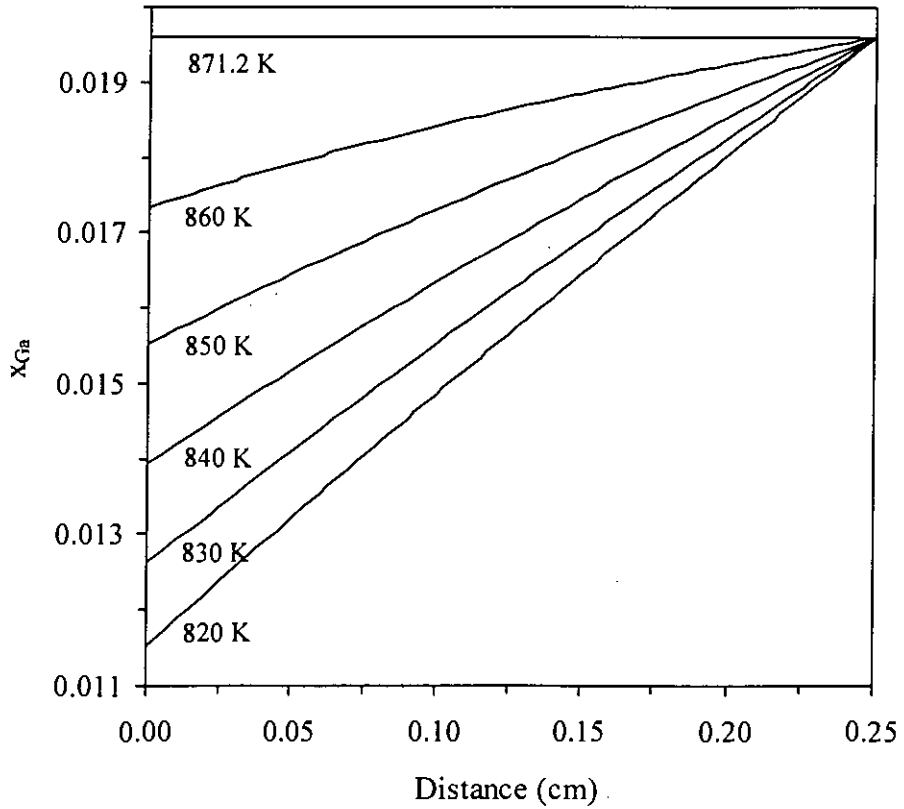
Figure 5.10: Atomic fraction profile of Ga atoms in In-rich solution during LPE growth at different growth temperatures for the given cooling rate of 0.5 K/min and equilibrium temperature T_E=871.2K for distances measured from solid liquid interface.
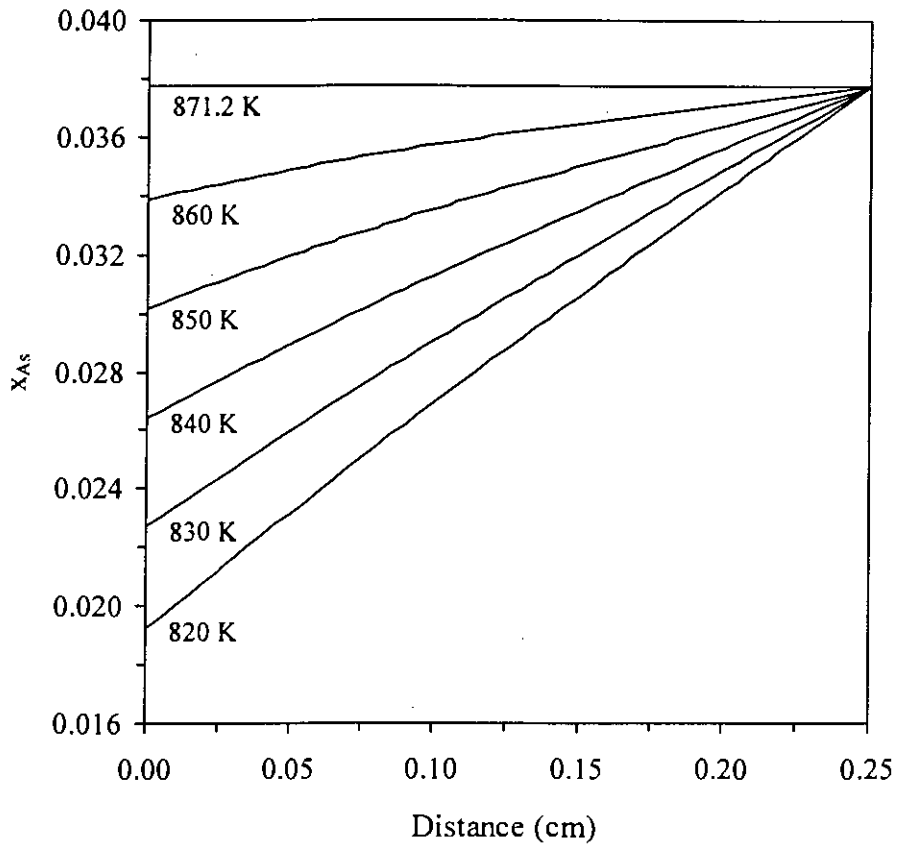
Figure 5.11: Atomic fraction profile of As atoms in In-rich solution at different growth temperatures for the given cooling rate of 0.5 K/min and equilibrium temperature T_E=871.2K for distances measured from solid liquid interface.

Figure 5.12: Dimensionless concentration profile of Ga in front of the crystal growing interface at different growth time for cooling rate of 1K/min and $T_E=871.2K$
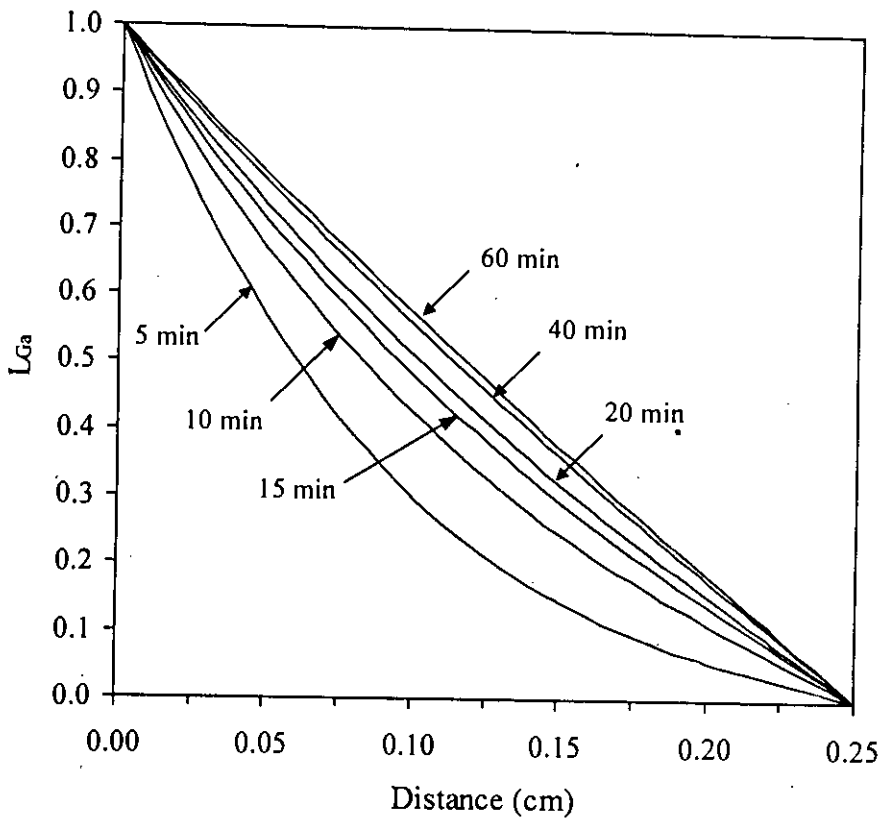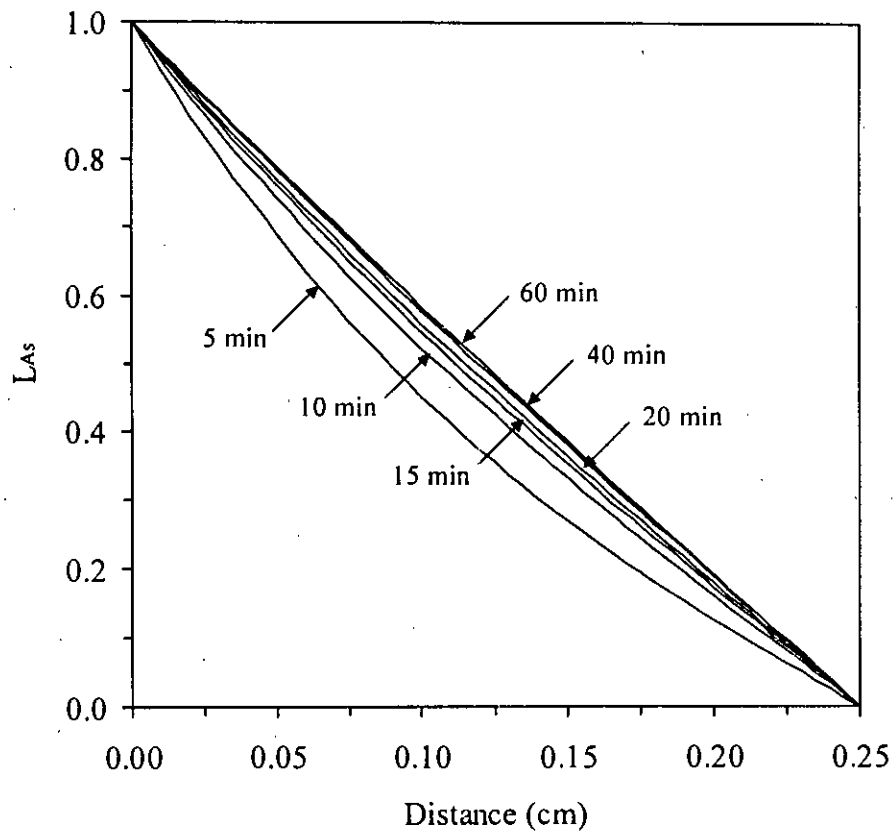
Figure 5.13: Dimensionless concentration profile of As in front of the crystal growing interface at different growth time for cooling rate of 1K/min and T_E=871.2K

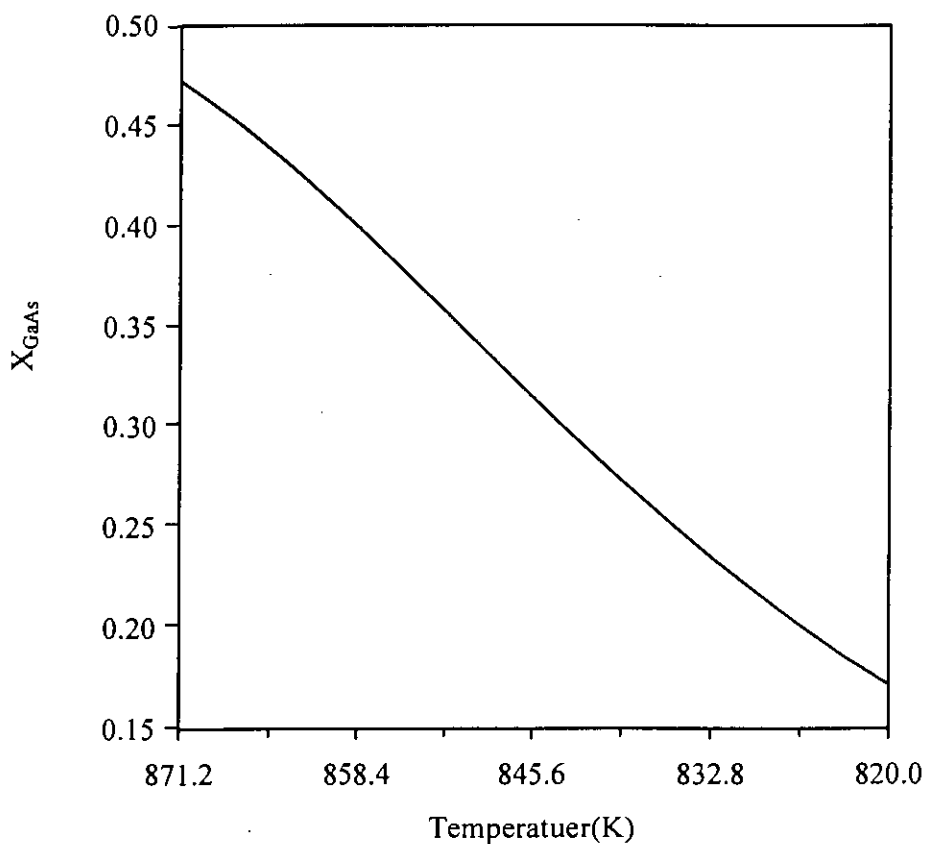**Figure 5.14:** Calculated values of GaAs solid mole fraction in the InGaAs alloy as a function of temperature for T_E=871.2K and cooling rates of 0.25K/min, 0.50K/min, 0.75K/min and 1K/min.
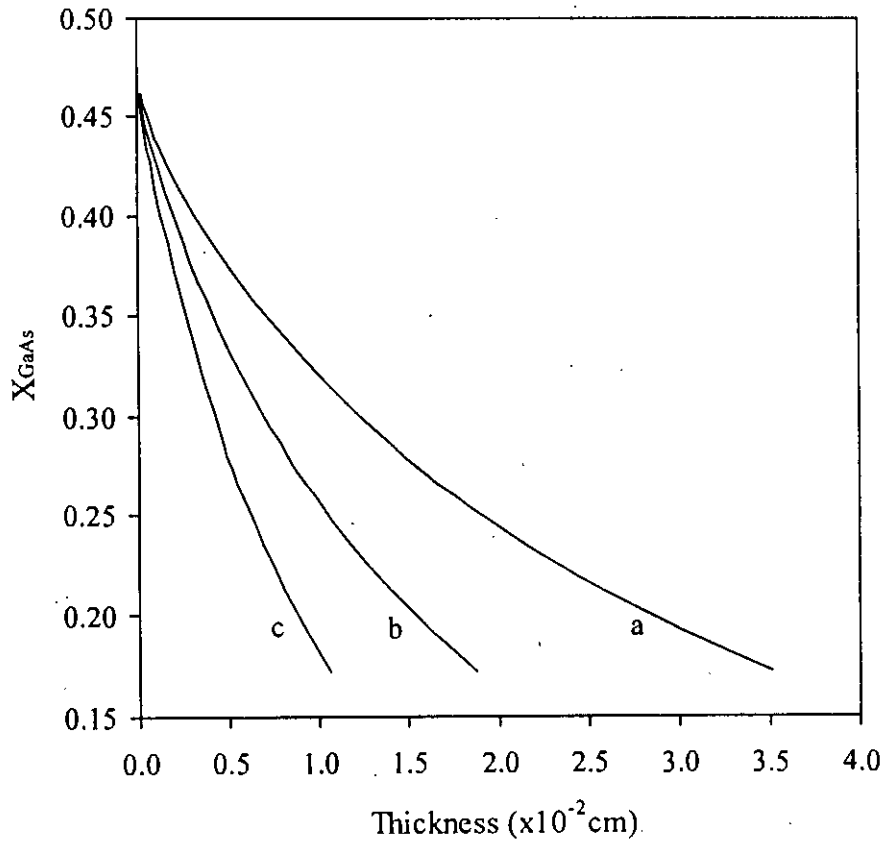
Figure 5.15: Simulated values of GaAs solid mole fraction in InGaAs alloy as a function of thickness of the grown layer for different cooling rates of: a) 0.25K/min, b) 0.5K/min and c) 1.0K/min for T_E=871.2K and T_{END}=867.9K
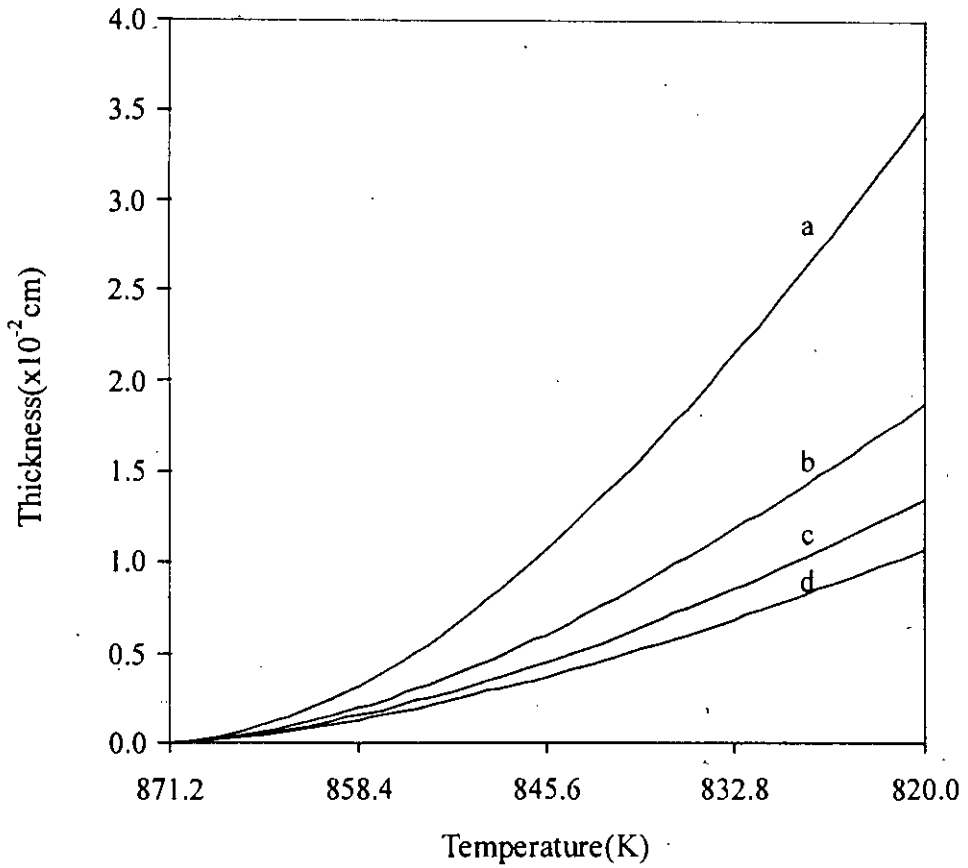
Figure 5.16: Thickness grown as function of temperature for various cooling rates of: a) 0.25K/min, b) 0.5K/min, c) 0.75K/min and d) 1.0K/min for T_E=871.2K with the ending point of each curve corresponding to T_{END}=820K.

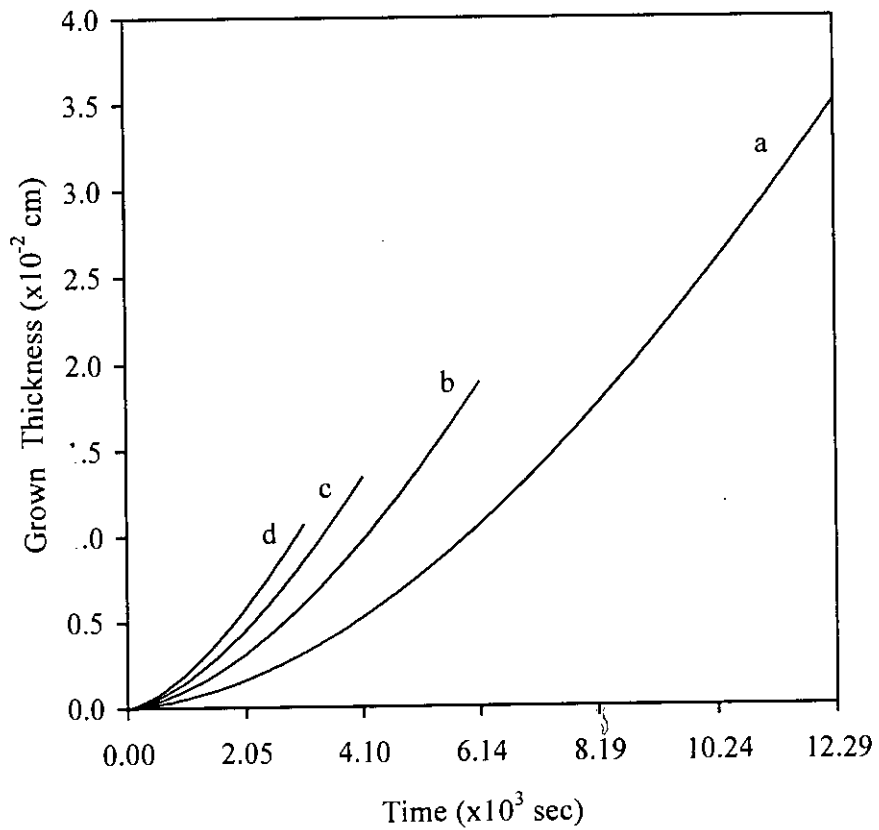**Figure 5.17:** Thickness grown as function of time for different cooling rates of: a) 0.25K/min, b) 0.5K/min, c) 0.75K/min and d) 1.0K/min for T_E=871.2K with the ending point of each curve corresponding to T_{END}=820K.

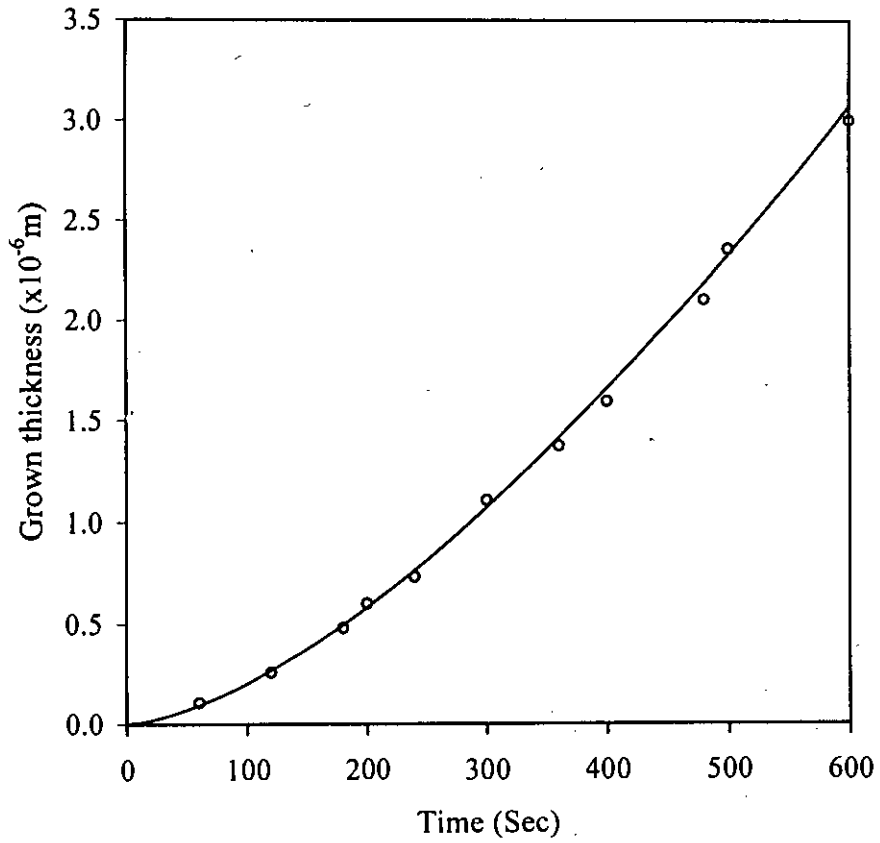**Figure 5.18:** Comparison between the theoretically evaluated values and experimentally reported values for T_E=871.2K and cooling rate of 0.33K/min. (o Ref. Kuphal 1994;(—) present work).

Figure 5.18 shows the comparison of the theoretical findings in this work with the reported work of Kuphal (1994) for the same initial experimental conditions as: atomic fraction of Ga, x_{Ga}=0.0196; atomic fraction of As, x_{As}=0.0377; cooling rate=0.33K/min and equilibrium temperature T_E=871.2K. The comparison shows a good agreement between present study and the reported values.

5.4 Indium Arsenide Phosphide (InAs$_x$P$_{1-x}$)

According to reported literature (Panish and Ilegems 1972), the initial atomic fraction of arsenic (As) atoms in InAsP LPE has been taken as 0.02 at the equilibrium temperature T_E=1073K and coefficient β as well as Δx_P^* have also been calculated from the reported isotherm liquidus curve. The temperature dependent diffusion coefficient of As and P in In-rich melt have been given by D_{As}=2.67×10^{-3} exp (-3440/T) cm^2/sec and D_P=18.23 exp (-11450/T) cm^2/sec (Pan et al 1986).

The following expression has been developed for atomic fraction of P, x_P as a function of atomic fraction of As, x_{As} and the temperature T from the InAsP ternary phase diagram (Panish and Ilegems 1972).

$$x_P=\exp(8.095107-1.201231\times10^4/T)\times\exp(-7.80937x_{As}) \qquad 5.6$$

Using the phase diagram (Panish and Ilegems 1972), an equation for solid mole fraction of InAs, X_{InAs} as a function of atomic fraction of As, x_{As} in liquid phase and the temperature T as

$$X_{InAs}=\exp(-28.24232+1.879563\times10^4/T+8.3937\times10^{-3}T)\times$$

$$\exp(-3.44046\times10^{-2}/x_{As}+9.0953x_{As}) \qquad 5.7$$

The value of atomic fraction of As, x_{As} for the next successive time increment in the InAsP LPE growth can be calculated from the equation 4.27.The equations 4.4, 4.27, 5.6 and 5.7 are used to simulate the atomic fraction profiles of solute (As and P) atoms in front of the growing crystal interface.

5.4.1 Results and discussion

The atomic fraction profiles of As and P atoms have been simulated one dimensionally in front of the growing crystal interface and are shown in figures 5.19 and 5.20 respectively for different growth temperatures. It is seen that at the lower temperatures the atomic fraction profiles of As and P atoms are more linear i.e. with higher slopes.

Figure 5.21 gives the variation of solid composition of InAs as a function of temperature. No significant difference was seen when the same parameter was calculated for any one of the four different cooling rates (0.25K/min, 0.5K/min, 0.75K/min and 1K/min). Figure 5.22 displays the results of the simulated solid mole fraction as a function of thickness of the grown layers for different cooling rates. It is observed that for a particular InAs solid mole fraction, applying the lower cooling rate could grow a thicker layer. The simulated thickness of the grown layers as a function of temperature for different cooling rates have been presented in figure 5.23. It shows that for a certain level of growth temperature (T_{END}=1023K), the thickness of the grown layer is lower for higher cooling rate due to the shorter time available for the growth. The average thickness of the grown InAsP calculated as a function of time for four different cooling rates with an ending temperature T_{END}=1023K as shown in figure 5.24. It is seen that for a

particular growth time, more rapid growth occurs for the solution, which are more rapidly cooled.

Figure 5.25 and 5.26 shows the dimensionless concentration profile of As and P atoms respectively in the melt at different growth time with a cooling rate of 1K/min. It is seen that the curves for lower growth time more distinguishable from each other in the case of As than in the case of P, which may be attributed to the faster saturation of As atoms in the melt at lower growth time.

The result obtained from the present theoretical model has been compared with the reported (Panish and Illegems 1972) results under same experimental conditions and are shown in figure 5.27. A good agreement is found between these theoretical findings and the reported values.

In figure 5.28, thickness grown for InAsP, InGaP and InGaAs from their equilibrium temperatures 1073K, 1103K and 871.2K respectively for 6×10^3 seconds with a cooling rate of 0.5K/min. Here it is found that thickness is grown faster in case of InAsP than other two ternaries. It is observed that diffusion coefficients for three ternaries are - for InGaP: $D_P = 2.26698 \times 10^{-4} cm^2/sec$, $D_{Ga} = 2.096437 \times 10^{-4} cm^2/sec$, for InGaAs: $D_{As} = 8.9 \times 10^{-5} cm^2/sec$, $D_{Ga} = 3.7 \times 10^{-5} cm^2/sec$ and for InAsP $D_{As} = 1.081879 \times 10^{-4} cm^2/sec$, $D_P = 4.230808 \times 10^{-4} cm^2/sec$ at their equilibrium temperatures. It is found that diffusion coefficient of As in InAsP is higher than that of InGaAs. Also diffusion coefficient of P in InAsP is higher than that of InGaP. This higher diffusion coefficient of solutes in InAsP may be the reason for faster growing of InAsP than other two ternaries.
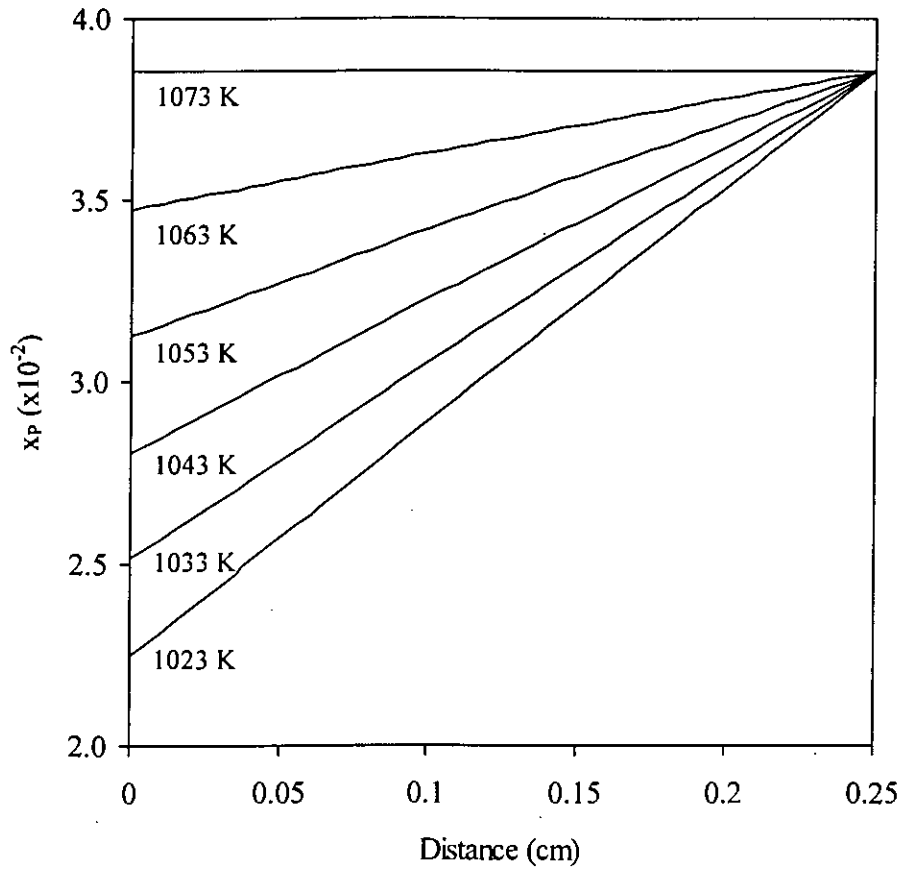
Figure 5.19: Atomic fraction profile of P atoms in the InAsP solution at various growth temperatures for the given cooling rate of 0.5 K/min and equilibrium temperature T_E=1073K for distances measured from solid liquid interface.

Figure 5.20: Atomic fraction profile of As atoms in the InAsP solution at various growth temperatures for the given cooling rate of 0.5 K/min and equilibrium temperature T_E=1073K for distances measured from solid liquid interface.
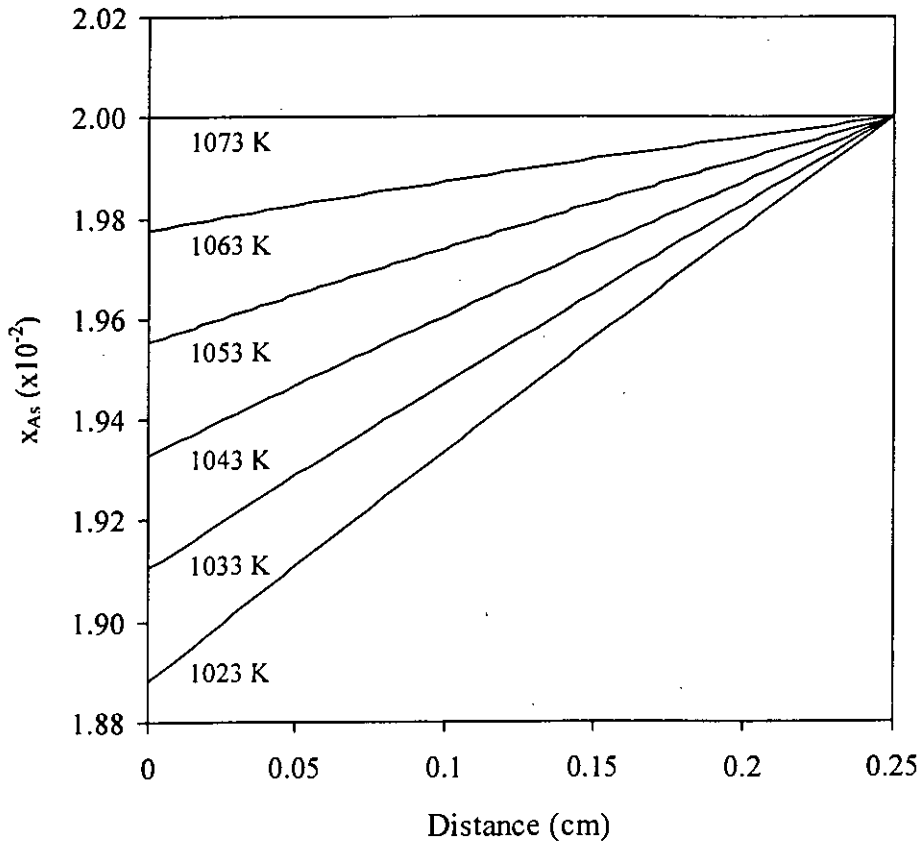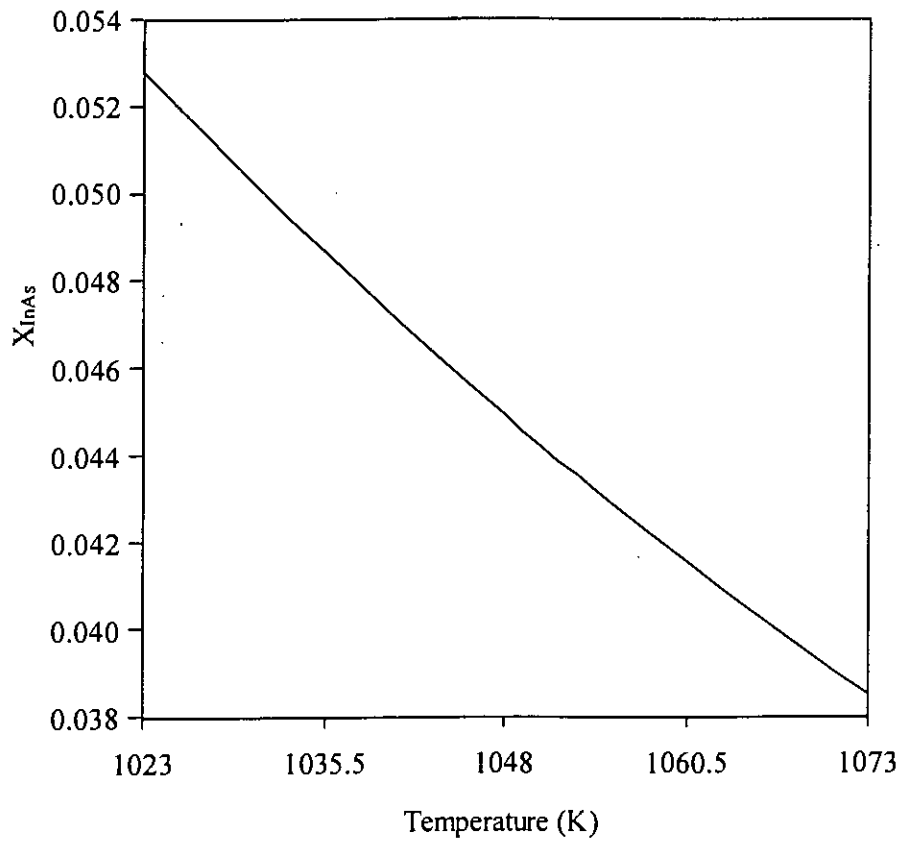
Figure 5.21: Calculated values of InAs solid mole fraction in the InAsP alloy as a function of temperature for T_E=1073K and cooling rates of 0.25K/min, 0.5K/min, 0.75K/min and 1K/min.
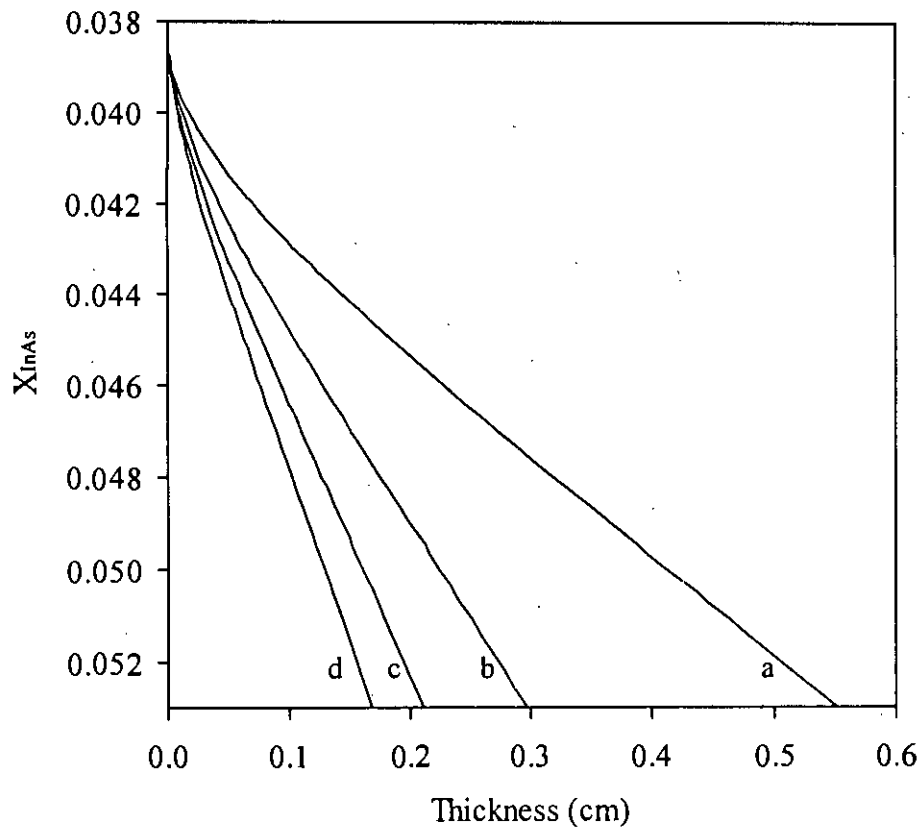
Figure 5.22: Simulated values of InAs solid mole fraction in InAsP alloy as a function of thickness of the grown layer for different cooling rates of: a) 0.5K/min, b) 1.0K/min, c) 1.5K/min and d) 2K/min for T_E=1073K with the ending point of each curve corresponding to T_{END}=1023K.
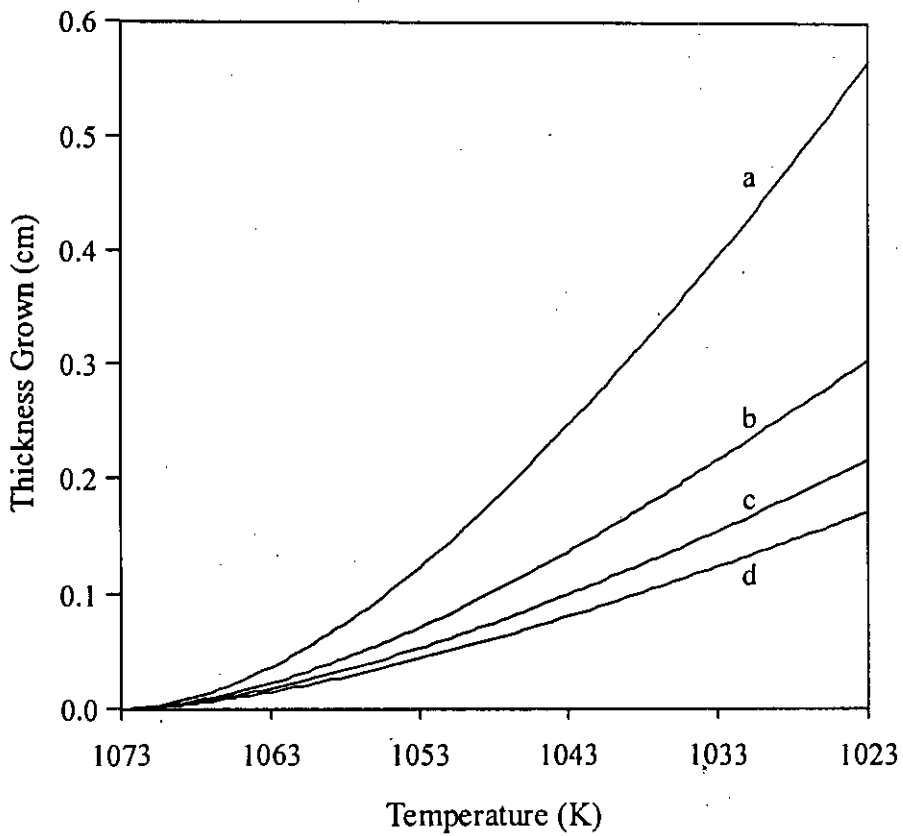
Figure 5.23: Thickness grown as function of temperature for various cooling rates of: a) 0.5K/min, b) 1.0K/min, c) 1.5K/min and d) 2K/min for T_E=1073K with the ending point of each curve corresponding to T_{END}=1023K.
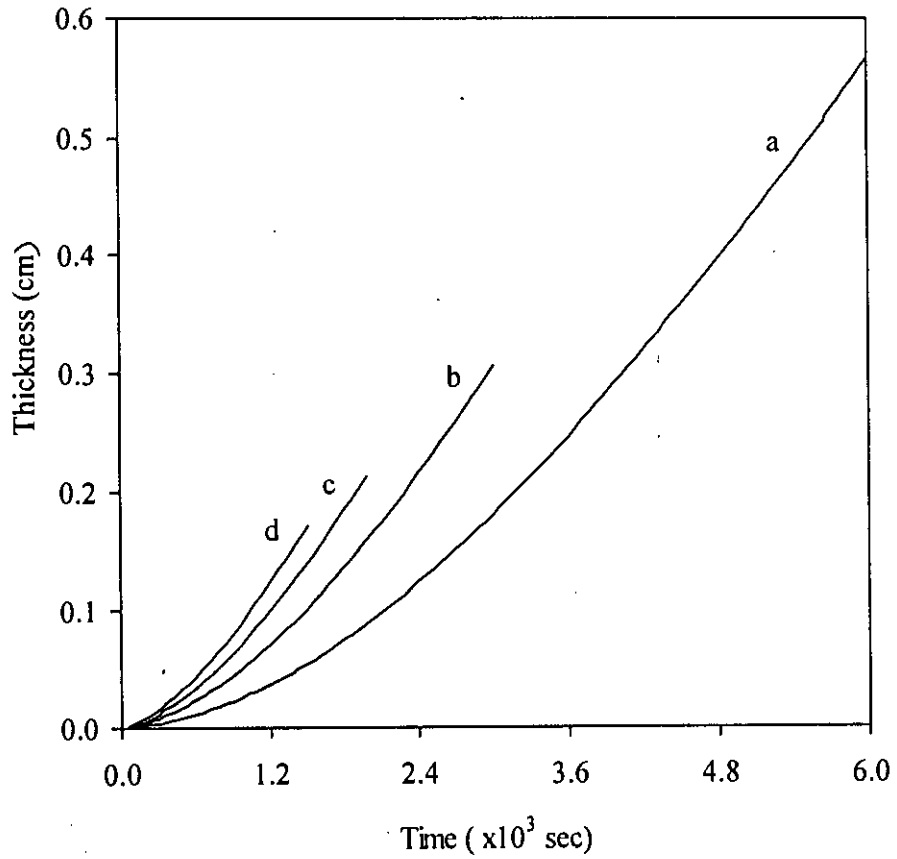
Figure 5.24: Thickness grown as function of time for different cooling rates of: a) 0.5K/min, b) 1.0K/min, c) 1.5K/min and d) 2K/min for $T_E=1073K$ with the ending point of each curve corresponding to $T_{END}=1023K$.
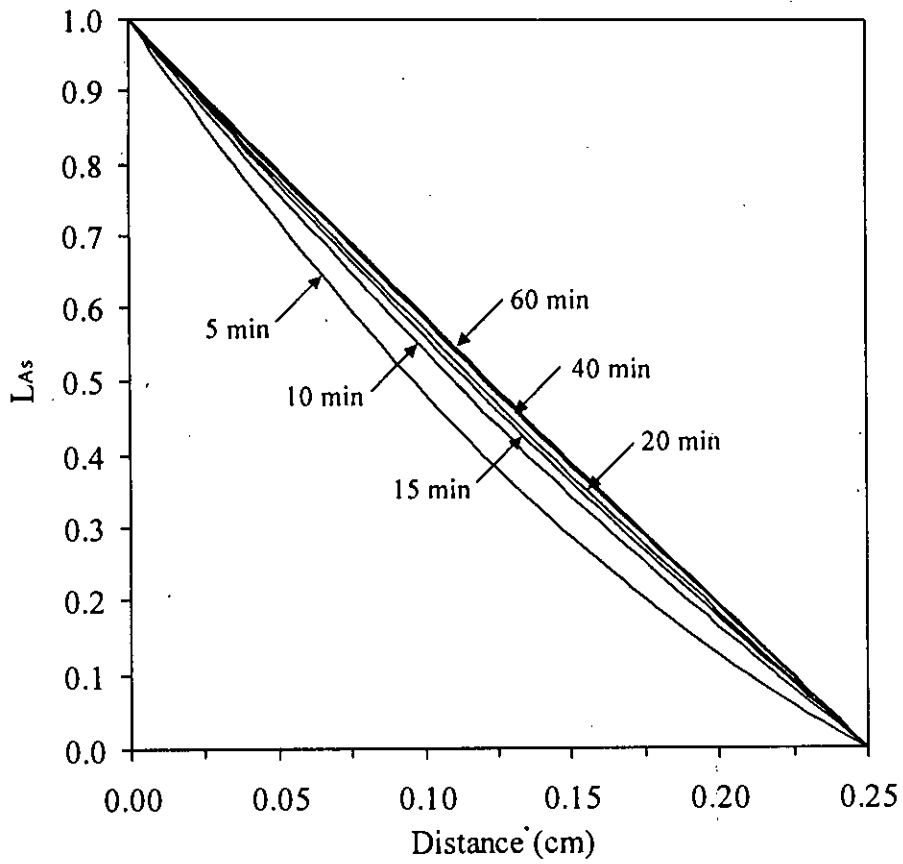
Figure 5.25: Dimensionless concentration profile of As in front of the crystal growing interface at different growth time for cooling rate 0.5 K/min and T_E=1073K
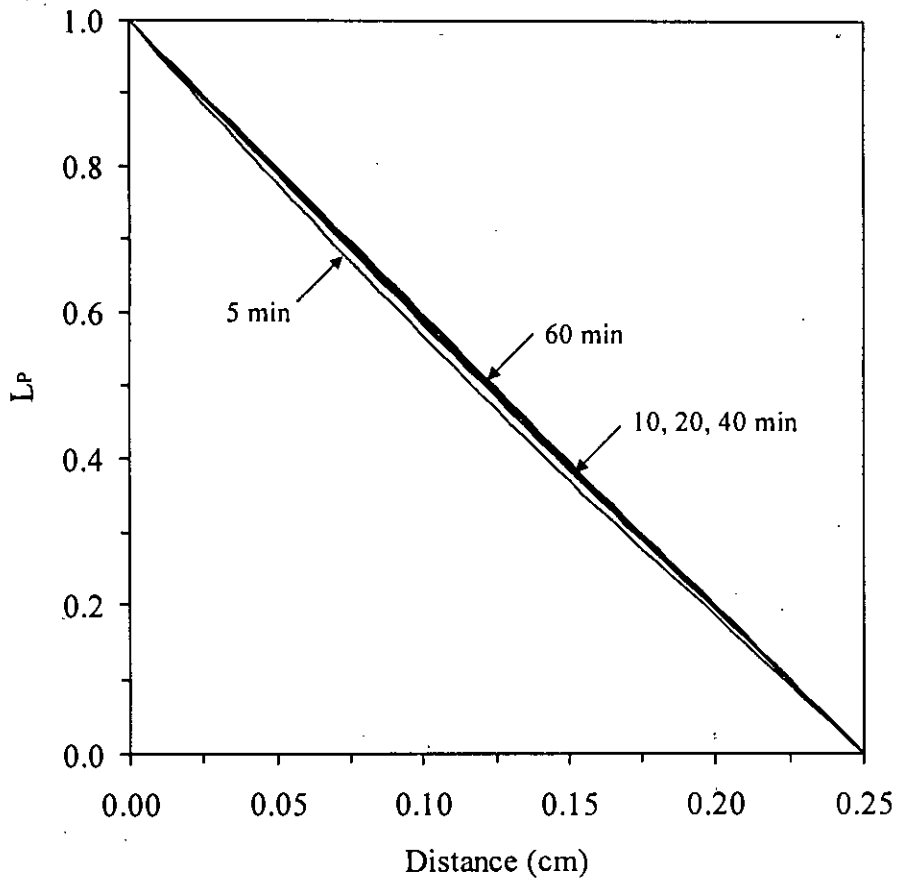
Figure 5.26: Dimensionless concentration profile of P in front of the crystal growing interface at different growth time for cooling rate 0.5K/min and T_E=1073K.
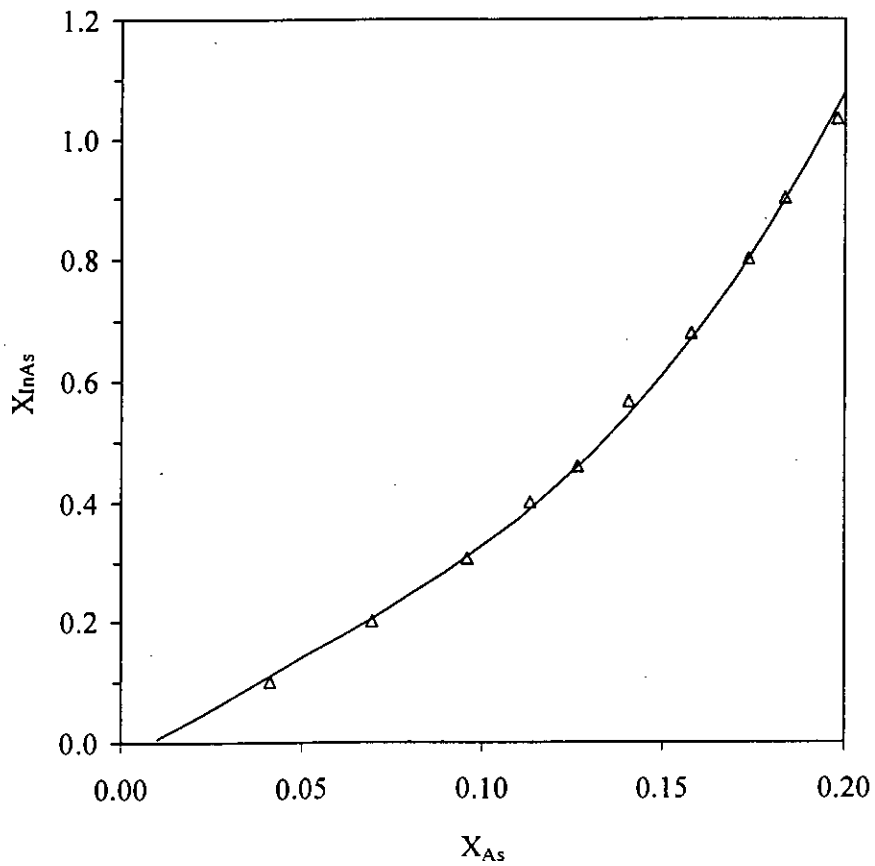
Figure 5.27: Comparison between our theoretical results and reported values of
isotherm curves for 1073K (Δ of Panish and Ilegems (1972) and (—)
the present work).
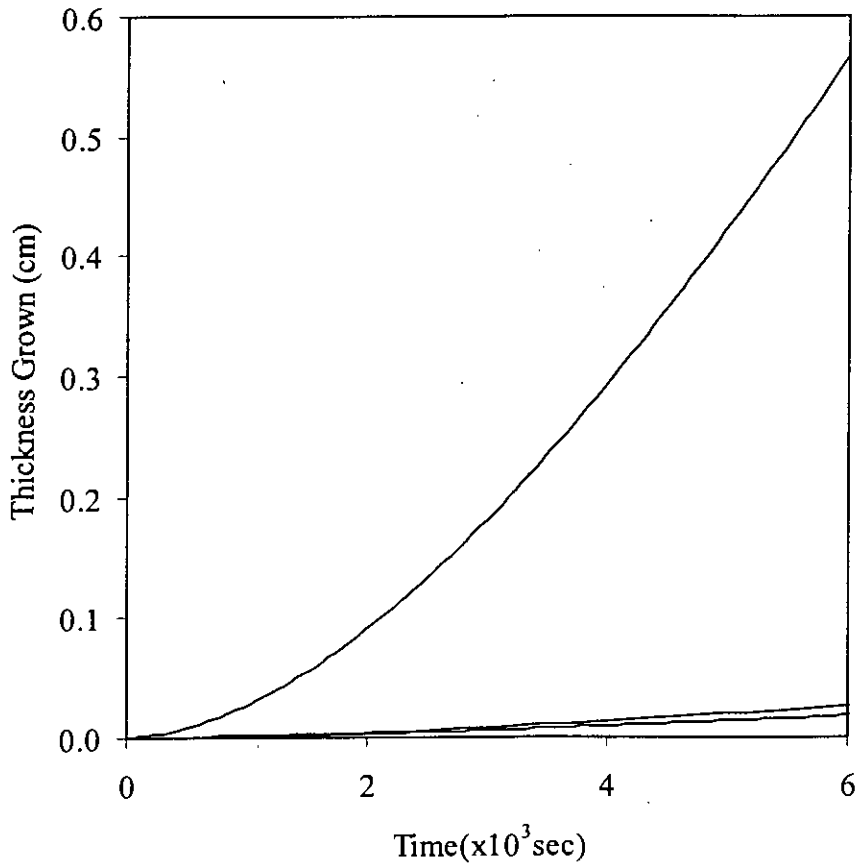
Figure 5.28: Thickness grown for InAsP, InGaP and InGaAs from their equilibrium temperatures 1073K, 1103K and 871.2K respectively for 6×10^3 second with a cooling rate of 0.5K/min.

5.5 Conclusion

The phase diagram and crystallization path are studied and are used to construct the concentration profiles of solute atoms along the distance perpendicular to the substrate in front of the growing crystal interface for $In_{1-x}Ga_xAs$, $In_{1-x}Ga_xP$ and $InAs_xP_{1-x}$ systems. The expression for equilibrium atomic fraction of solute atoms at the growing crystal interface has been developed with the help of reported phase diagrams. The equilibrium solute atoms at the next successive time increment has been expressed by the concept of fluxes, which is proportional to its constituent solid mole fraction at any time. The three ternaries are also compared for their thickness grown as a function of time from their respective equilibrium temperature for a fixed duration and a cooling rate.

The one dimensional computed data of the present study have been used to calculate the dimensionless parameter of concentration, average layer thickness as a function of time and temperature at different cooling rates Also the composition of the grown solid as a function of the layer thickness and growth temperature are observed.

The outcome of the study signifies that the concentration of the solute atoms decreases near the solid liquid interface as the growth proceeds. It is observed that the solid mole fraction depends on growth temperature but independent of cooling rates. But the grown layer thickness is affected by the cooling rates. Among the three ternaries, thickness of the layer grows faster for InAsP than the other two. A good agreement is found between our theoretical and available reported observations as they were compared.

References

Adams G.W., Schmitt, J.L. and Zalabsky, R.A. (1984), 'The homogeneous nucleation of nonane', J. Chem. Phys. Vol. 81, pp. 5074-5078.

AicheleT., Lorenz A., Hergt R., Görnert P. (2003), 'Garnet layers prepared by liquid phase epitaxy for microwave and magneto-optical applications – a review', Cryst. Res. Technol., Vol. 38, pp. 575 – 587.

Astles M.G. (1990), 'Liquid Phase Epitaxial Growth of III-V Compound Semiconductor Materials and their Device Applications', Adam Hilger, England.

Bauser, E., Frik, M., Loechner, K.S., Schmidt, L. and Ulrich, R. (1974). 'Substrate orientation and surface morphology of GaAs liquid phase epitaxial layers', J.Cryst. Growth, Vol. 27, pp. 148-153.

Benz K.W. and Bauser E. (1980), 'Grwoth of binary III-V semiconductors from metallic solution', Crystals, Vol. 3, Springer-Verlag, Berlin, Heidelberg, pp. 1-48.

Beppu T., Iwamoto M., Naito M. and Kasami A. (1977), 'High-efficiency GaP green LED's by zinc diffusion into an n-LPE layer', IEEE Trans. Electron. Devices, Vol. ED-24, pp. 951-955.

Berger S., Quoizola S., Fave A., Ouldabbes A. , Kaminski A., Perichon S., Chabane-Sari N-E. , Barbier D., Laugier A. (2001), 'Liquid Phase Epitaxial Growth of Silicon on Porous Silicon for Photovoltaic Applications', Cryst. Res. Technol., Vol. 36, pp. 1005–1010.

Casey Jr. H.C. and Panish M.B. (1978), 'Heterostructure lasers, Part B: Materials and Operation Characteristics, Academic press, New York, pp. 71-155.

Chen C.W. and Wu M.C. (1995), 'Liquid phase epitaxial growth and characterization of InGaAsP layers grown on GaAsP substrates for applications to orange light –emitting diodes', J.Appl. Phys., Vol. 77, pp. 905-909.

Chernov A.A. (1984), 'Modern crystaaolgraphy III', Springer Veriag, Berlin, Germany, pp. 48-103.

Crossley I. and Small M.B. (1971), 'Computer Simulation of Liquid Phase Epitaxy of GaAs in Ga solution', J.Cryst. Growth, Vol. 11, pp. 157-165.

Crossley I. and Small M.B. (1972), 'The application of numerical methods to simulate the Liquid Phase Epitaxial growth of $Ga_{1-x}Al_xAs$ from an unstirred solution', J.Cryst. Growth, Vol. 11, pp. 157-165.

Dizaji H.R. and Dhanasekaran R. (1996a), 'A theoretical approach to the $In_{1-x}Ga_xP$ LPE growth by computer simulation technique', Phys. stat. soli. (a), Vol. 156, pp. 71-79.

Dizaji H.R. and Dhanasekaran R. (1996b), 'Simulation studies of liquid phase epitaxial growth of $In_{1-x}Ga_xAs$', Mater. Sci. and Engg. B, Vol. 39, pp. 117-122.

Dizaji H.R. and Dhanasekaran R. (1996c), 'Concentration profile and growth rate studies of $In_{1-x}Ga_xP$ LPE by computer simulated technique', Mater. Sci. :Mater. Sci. Electronics, Vol. 7, pp. 181-185.

Dobosz D. and Zytkiewicz Z.R. (1991), 'Diffusion limited LPE growth of $Ga_xIn_{1-x}P$ on (100) GaAs', Phys. Stat. Solid. (a), Vol. 128, pp. 123-127.

Dutartre D. (1983), 'LPE growth rate in $Al_xGa_{1-x}As$ system; Theoretical and Experimental Analysis', J. Cryst. Growth, Vol. 64, pp. 268-274.

Dutta N.K., Wessel T., Olsson N.A.., Logan R.A., Koszi L.A. and Yen R. (1985), 'Fabrication and performance characteristics of 1.55 µm InGaAsP on (100)-InP for 1.15-1.31 µm spectral region', Appl. Phys. Lett., Vol. 46, pp. 525-527.

Feng M., Cook L.W., Tashima M.M. and Stillman G.E. (1980), 'Lattice constant, band gap, thickness and surface morphology of InGaAsP-InP layers grown by step-cooling, equilibrium-cooling, super-cooling and two-phase cooling growth techniques', J. Electron. Mater. Vol. 9, pp. 241-281.

Gao H.H., Krier A. and Sherstnev V.V. (1999), 'High quality InAs grown by liquid phase epitaxy using gadolinium gettering', Semicond. Sci. Technol. Vol. 14, pp. 441–445.

Greene P.D., Prins A.D., Dunstan D.J. and Adams A.R. (1987), 'Indium phosphide and quaternary doping superlattice grown by liquid phase epitaxy', Electron. Lett., Vol. 23, pp. 324-325.

Horikoshi L. (1986), 'The Physics and Fabrication of Micro-structure', Les Houches.

Hossain MD. M., Dhanasekaran R. and Ramasamy P. (1999), 'Concentration profile Surfaces and Contour Studies of GaSb by LPE using simulation Technique', Mater. Sci. and Engg. B., Vol. 64, pp 161.

Hossain Md. Mostak (1999a), 'Theoretical Investigation on the Growth kinetics of Compound Semiconductors' Ph.D. Thesis, Alagappa University, Karaikudi, India.

Hsieh J.J., Rossi J.A. and Donnelly J.P.(1976), 'Room temperature cw operation of GaInAsP/InP double hetero-structure diode lasers emitting at $1.1\mu m$', Appl. Phys. Lett. Vol. 28, pp. 709-711.

Kanai H. Kimura M., Dost. S., Tanaka A. and Sukegawa T. (1997), 'Gravity effect on dissolution and growth of GaSb by liquid phase epitaxy', J. Cryst. Growth, Vol. 174, pp. 226-229.

Kao Y.C. and Eknoyan O. (1983), 'Thickness of GaP liquid phase epitaxial layers grown by step-cooling, equilibrium-cooling and ramp-cooling methods', J. appl. Phys., Vol. 54, pp. 1865-1867.

Katz J., Bar-Chaim N., Chen P.C., Margalit S., Ury I. Wilt D., Yust M. and Yariv A. (1980), 'A monolithic integration of GaAs layers with a new technique', J. Cryst. Growth, Vol. 42, pp. 321-327.

Kaufmann L.M.F. and Heim K. (1977), 'A new graphite boat construction for the LPE growth of thin GaAs layers with a new technique', J. Cryst. Grwoth, Vol. 42, pp. 321-327.

Kimura M., Djilali N. and Dost S. (1994), 'Convective transport and interface kinetics in liquid phase epitaxy', J. Cryst. Growth, Vol. 143, pp.334-348.

Konig U. and Jorke H. (1985), 'Periodic doping and hetero-structure multilayers of $Ga_xIn_{1-x}As_yP_{1-y}$: LPE growth and characterization,' J. Cryst. Growth, Vol. 73, pp. 515-522.

Körber W. and Benz K.W. (1985), 'Low temperature growth and thermodynamic and photoluminescence properties of LPE $In_{1-x}Ga_xP$ layers', J. Cryst. Growth, Vol. 73, pp. 179-186.

Kressel H. and Nelson H. (1973), 'Properties and application on III-V compound films deposited by liquid phase epitaxy', Eds. By Hass G., Francombe M.H. and Hoffman R.W., Physics of Thin films, Academic press, New York, Vol. 7, pp. 115-256.

Krier A. and Mao Y. (1995), 'Electrical transport properties and photoluminescence of lattice-matched $InAs_{0.91}Sb_{0.09}$ on GaSb grown by liquid phase epitaxy', Semicond. Sci. Technol., Vol. 10, pp. 930-936.

Kuphal E. (1991), 'Liquid Phase Epitaxy ', Appl. Phys. A, Vol.52, pp.380-409.

Kuphal E. (1994), 'Liquid Phase Epitaxy of III-V compounds', Current Topics in Cryst. Growth Res., Vol.1, pp. 47-82.

Kuphal E.(1984), 'Phase diagrams of InGaAsP, InGaAs and InP lattice matched to (100) InP', J. Cryst. Growth, Vol. 67, pp.441- 457.

Leheny R.F., Nahory R.E. and Pollack M.A. (1979), '$In_{0.53}Ga_{0.47}As$ pin photodiodes for long wavelength fibre optic systems', Electron. Lett., Vol. 15, pp. 713-715.

Mariette H., Thierry-Mieg V., Etcheberry A., Guillaume J.C., Marbeuf A. and Rommeluere M. (1981), 'Composition profiles and growth kinetics of $GaxIn1-xP$ LPE layers: Experimental and theoretical approach', J.Cryst. Growth, Vol. 53, pp. 413-417.

Michael B.B. (1965), 'Nucleation process' in 'Energetics in Metallurgical phenomena' Eds. William M. Mueller, Gordon and Breach Science Publishers, United Kingdom', Vol. I, pp. 111-160.

Milanova M., Mintairov A., Rumyantsev V. and Smekalin K. (1999), 'Spectral characteristics of GaAs solar cells grown by LPE', J. Elect. Mater. Vol. 28, pp 35-38.

Moon R.L. (1974), 'The influence of growth solution thickness on the LPE layer thickness and constitutional super-cooling requirement for diffusion-limited growth', J. Cryst. Growth, Vol. 27, pp. 62-69.

Morrison C.B. and Bedair S.M. (1982), 'Phase diagram of the InGaP ternary system', J. Appl. Phys., Vol. 53, pp. 9058-9062.

Nelson H. (1963), 'Epitaxial growth from the liquid state and its application to the fabrication of tunnel and laser diodes', RCA Rev. Vol. 24, pp. 603-615.

Ohki Y., Shimomura K., Kikugawa T., Ravikumar K.G., Izumi A., Arai S. and Suematsu Y. (1987), 'Electric field-induced absorption in GaInAsP/InP MQW structures grown by LPE', Jpn. J. Appl. Phys., Vol. 26, pp. L579-L581.

Olchowik J.M. (1994), 'Influence fo the interface on contact supersaturation of GaInPAs alloys', Phys. Stat. Solid. (a), Vol 146, pp. K19-K22.

Pan N., Tabatabaie N. and Stillman G.E.(1986), 'LPE diffusion limited growth of InGaAs', J. Cryst. Grwoth, Vol. 78, pp. 97-104.

Panish M.B. and Ilegems M. (1972), 'Phase equilibrium in ternary III-V systems', Ed. Reiss H. and Mc Caldin J.O., Progr. in solid-state Chem. Pergamon, Oxford, Vol. 7, pp. 39-83.

Panish M.B., Hayashi I. And Sumski S. (1970), 'Double-heterostructure injection lasers with room-temperature thresholds as low as 2300 A/cm^2 ',Appl. Phys. Lett., Vol. 16, pp. 326-328.

Parry M.K. and Krier A. (1994), 'Efficient 3.3µm light emitting diodes for detecting methane gas at room-temperature', Electronics Letters, Vol. 30, pp. 1968-1969.

Peev N.S., 'Some Phase Boundary Region Correlation in the Liquid Phase Epitaxy Growth Process', Cryst. Res. Technol., Vol-34, No 6, pp. 851-858.

Petzow G. and Effenberg G. (1992), 'Ternary alloys', VCH Publishers, New York, Vol. 5.

Richard Haberman (1987), 'Elementary Applied Partial Differential Equations, 2nd Edition, Prentice Hall, INC.', New Jersey, pp. 478-518.

Sasai Y., Hase N., Ogura M. and Kajiwara T. (1986), 'Fabrication and lasing characteristics of 1.3µm InGaAsP multiquantum-well lasers', J. Appl. Phys., Vol. 59, pp. 28-31.

Stringfellow G.B. (1970), 'Calculation of the Ga-In-P ternary phase diagram using the Quasi-chemical Equilibrium', J. Electrochem. Soc. Vol. 117, pp. 1301-1335.

Stringfellow G.B. (1982), 'Epitaxy', Rep. Prog. Phys. Vol. 45, pp. 469-525.

Sukegawa T., Kimura M. and Tanaka A. (1988), 'Gravity effect on dissolution and growth of silicon in the In-Si system', J. Cryst. Growth, Vol. 92 pp. 46-52.

Sun Y.M., Jiang W.J. and Wu M.C. (1996), 'Optical properties of GaSb alloys and photodiodes grown by liquid phase epitaxy', J.Appl. Phys., Vol. 80, pp. 1731-1734.

Tanaka S., Takamatsu H., Hiramatsu K. and Akasaki I. (1989), 'LPE growth of InGaP/InGaAsP multiple thin layers on (111)A GaAs substrate', J. Cryst. Growth, Vol. 98, pp. 653-658.

Traeger G., Kuphal E., Zschauer K.H. (1988), 'Diffusion limited LPE growth of mixed crystals: application to $In_{1-x}Ga_xAs$ on InP', J. Cryst. Growth. Vol. 88, pp. 205-214.

Vaya P.R. (1989), 'Introduction to Semiconductor Lasers', Semiconductor Device Research laboratory, I.I.T., Madras, India,pp. 46-56.

Wieder H.H., Clawson A.R. and McWiliams G.E. (1977), '$In_xGa_{1-x}As_yP_{1-y}$ / InP heterojunction photodiodes,' Appl. Phys. Lett., Vol. 31, pp. 468-470.

Wilcox W.R. (1982), 'Computer simulation of growth of thick layers from solution of finite solute concentration without convection', J. Cryst. Growth, Vol. 56, pp. 690-698.

Zhuravlev K.S., Shamirzaev T.S.and Yakusheva N.A. (1998), 'Properties of manganese-doped gallium arsenide layers grown by liquid phase epitaxy from a bismuth melt', Semiconductors, Vol. 32, pp. 704 -710.